Egy középső-triász karbonátos rétegsor a Szegedi-medencében: diagenetikus események a dolomitosodástól a szénhidrogén-felhalmozódásig

Garaguly István[1], Varga Andrea[1], Raucsik Béla[1], Schubert Félix[1], Czuppon György[2], Papp Nikoletta[1], Robert Frei[3]

[1]Szegedi Tudományegyetem Ásványtani, Geokémiai és Kőzettani Tanszék, Szeged
[2]MTA CSFK Földtani és Geokémiai Intézet, Budapest
[3]Department of Geosciences and Natural Resource Management, Univ. of Copenhagen

PROJECT FINANCED FROM THE NRDI FUND
MOMENTUM OF INNOVATION

MOL GROUP

Institute for Geological and Geochemical Research
Research Centre for Astronomy and Earth Sciences
Hungarian Academy of Sciences

UNIVERSITY OF COPENHAGEN

Motivation

The Szeged Dolomite Formation is the most common Triassic basement formation in the southern part of the Pannonian Basin in Hungary. This succession serves as good hydrocarbon reservoir in numerous cases and provides significant hydrocarbon production in this region. Nonetheless, the Szeged Dolomite reservoir rocks have not been investigated since early 90s.

This study was performed on 60 core samples representing 25 wells in the Szeged Basin.

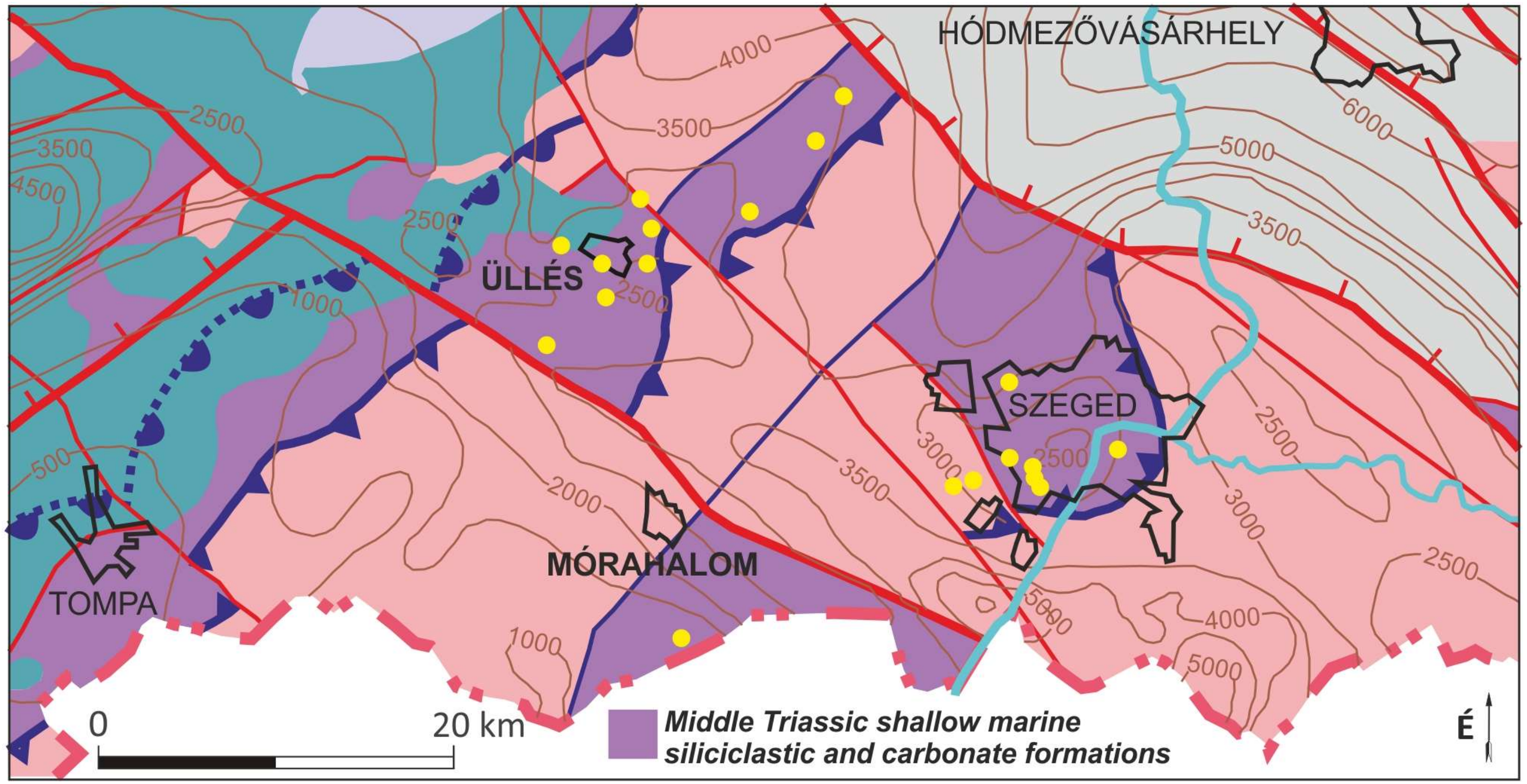

Basement formations of the Szeged Basin (Haas et al. 2010, modified)

Materials

Samples were collected from fractured and tectonically altered Middle Triassic dolostones, from reworked dolomite pebbles in the overlaying Miocene conglomerate, and from dolomite veins in the underlaying sandstone and metamorphites.

Methods

- Macroscopic description
(60 samples from 25 wells)
- Microscopic petrography
(50 samples, ~90 thin sections)

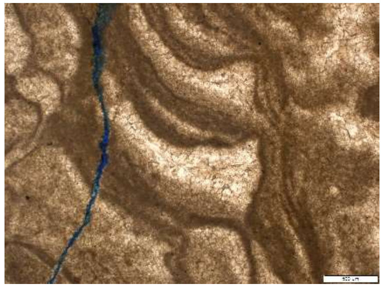

- Fluorescence microscopy

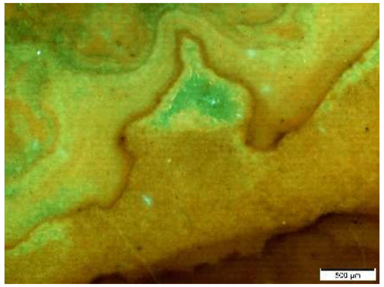

- Cathodoluminescence microscopy

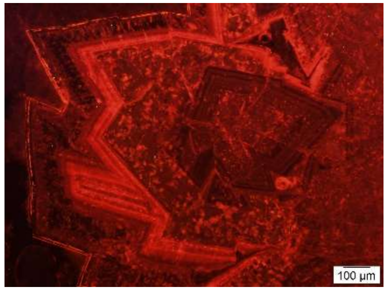

- Stable isotope (^{18}O and ^{13}C) geochemistry
(123 fabric-selected powdered samples)
- Radiogenic ($^{87}Sr/^{86}Sr$) isotope ratios
(20 samples)
- Fluid inclusion microthermometry
(20 samples, ~550 fluid inclusions)

- Raman microspectroscopy on fluid inclusions

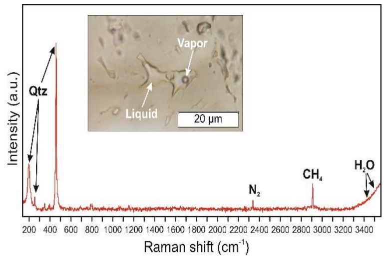

- Hydrogen isotope composition of fluid inclusion-hosted H_2O
(11 samples)

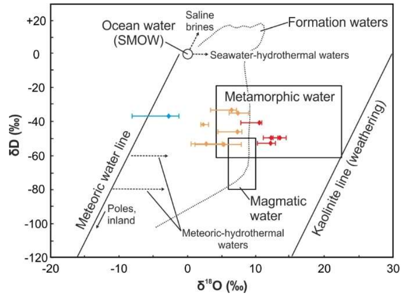

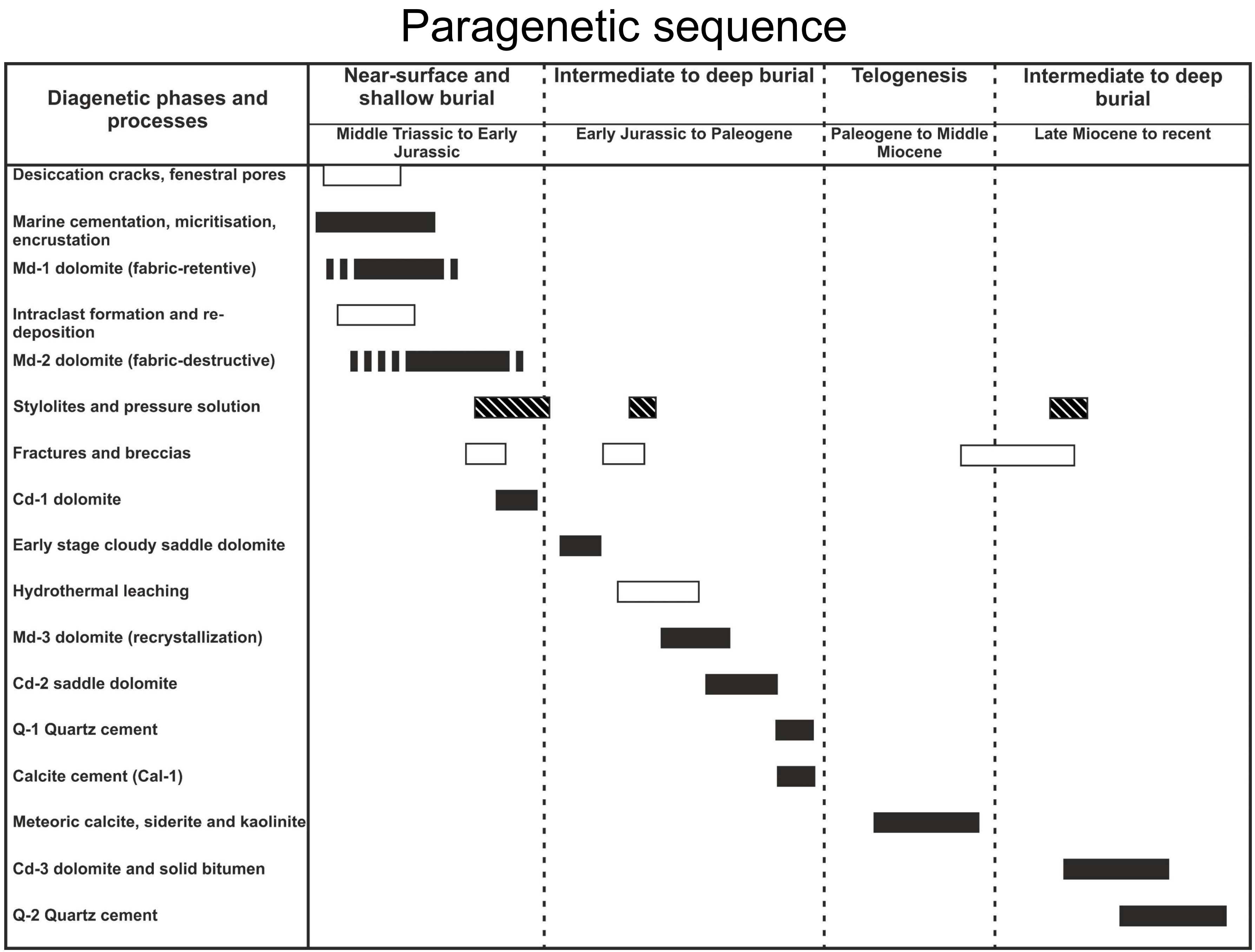
Paragenetic sequence
Diagenetic phases and processes
Near-surface and shallow burial
Intermediate to deep burial
Telogenesis
Intermediate to deep burial
Middle Triassic to Early Jurassic
Early Jurassic to Paleogene
Paleogene to Middle Miocene
Late Miocene to recent
Desiccation cracks, fenestral pores
Marine cementation, micritisation, encrustation
Md-1 dolomite (fabric-retentive)
Intraclast formation and re-deposition
Md-2 dolomite (fabric-destructive)
Stylolites and pressure solution
Fractures and breccias
Cd-1 dolomite
Early stage cloudy saddle dolomite
Hydrothermal leaching
Md-3 dolomite (recrystallization)
Cd-2 saddle dolomite
Q-1 Quartz cement
Calcite cement (Cal-1)
Meteoric calcite, siderite and kaolinite
Cd-3 dolomite and solid bitumen
Q-2 Quartz cement

Depositional textures and early diagenetic processes

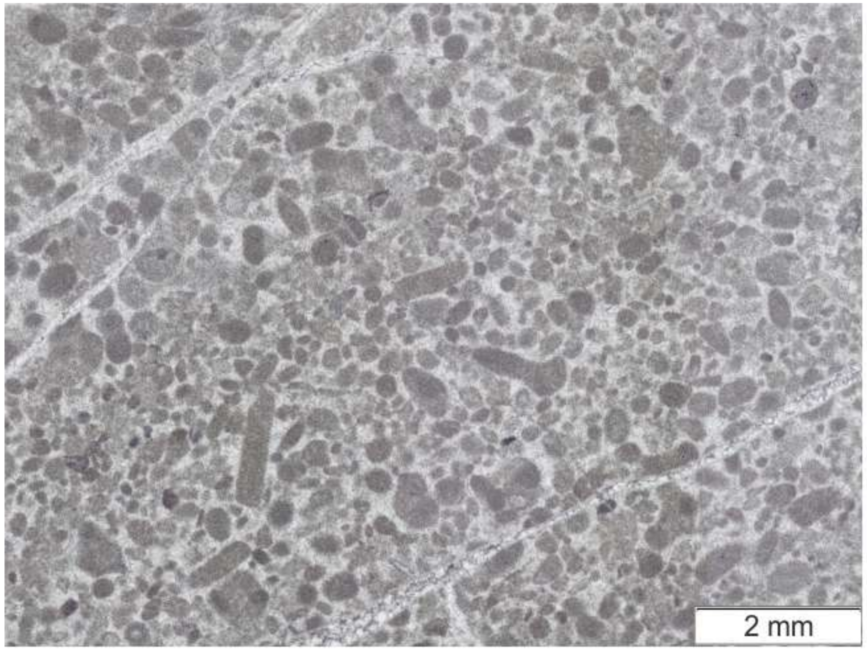

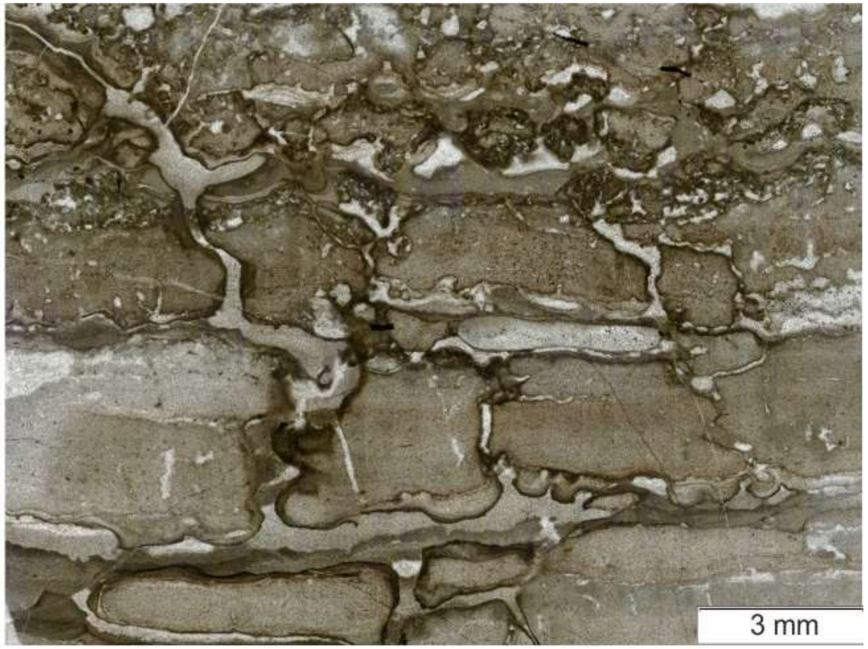

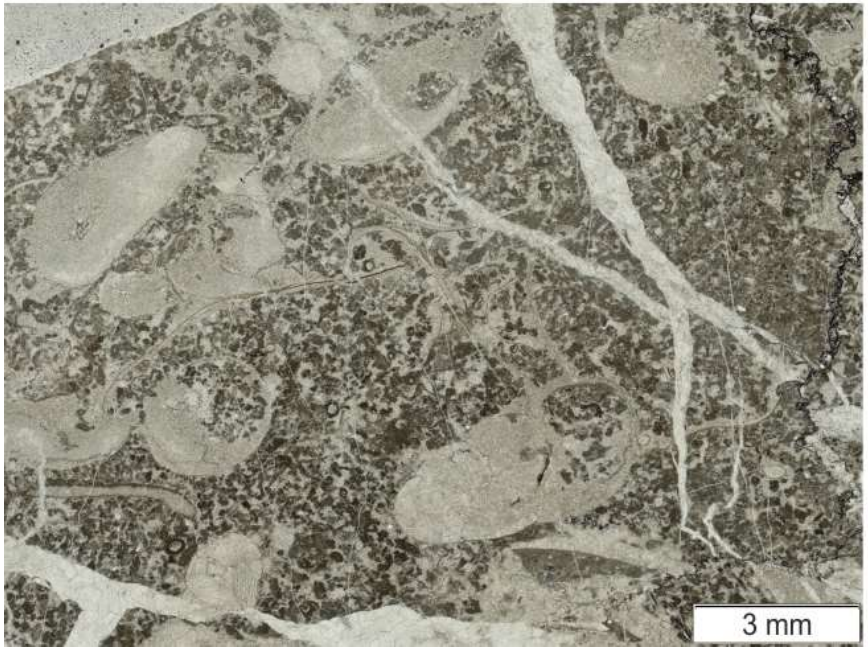

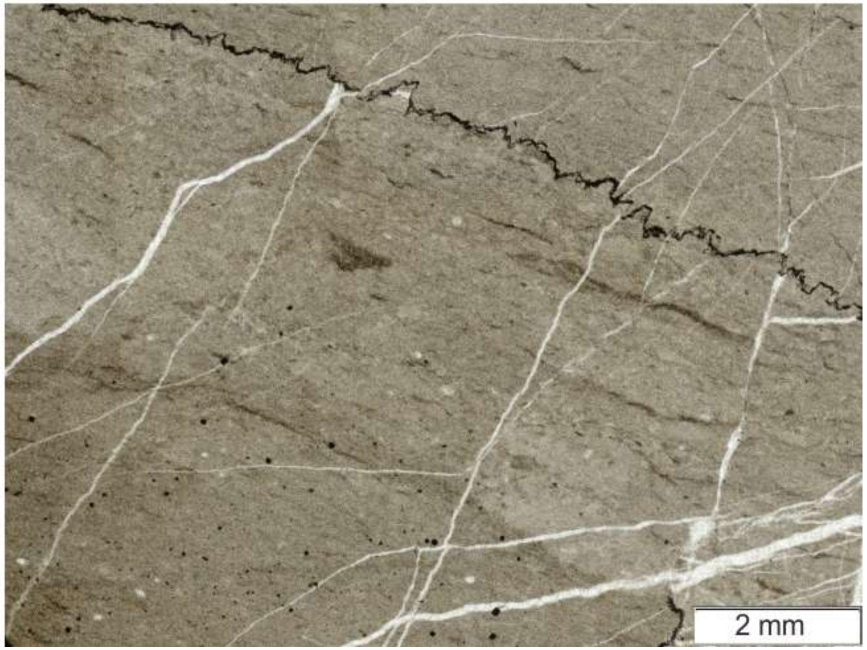

Secondary porosity due to Late Cretaceous leaching and recrystallization

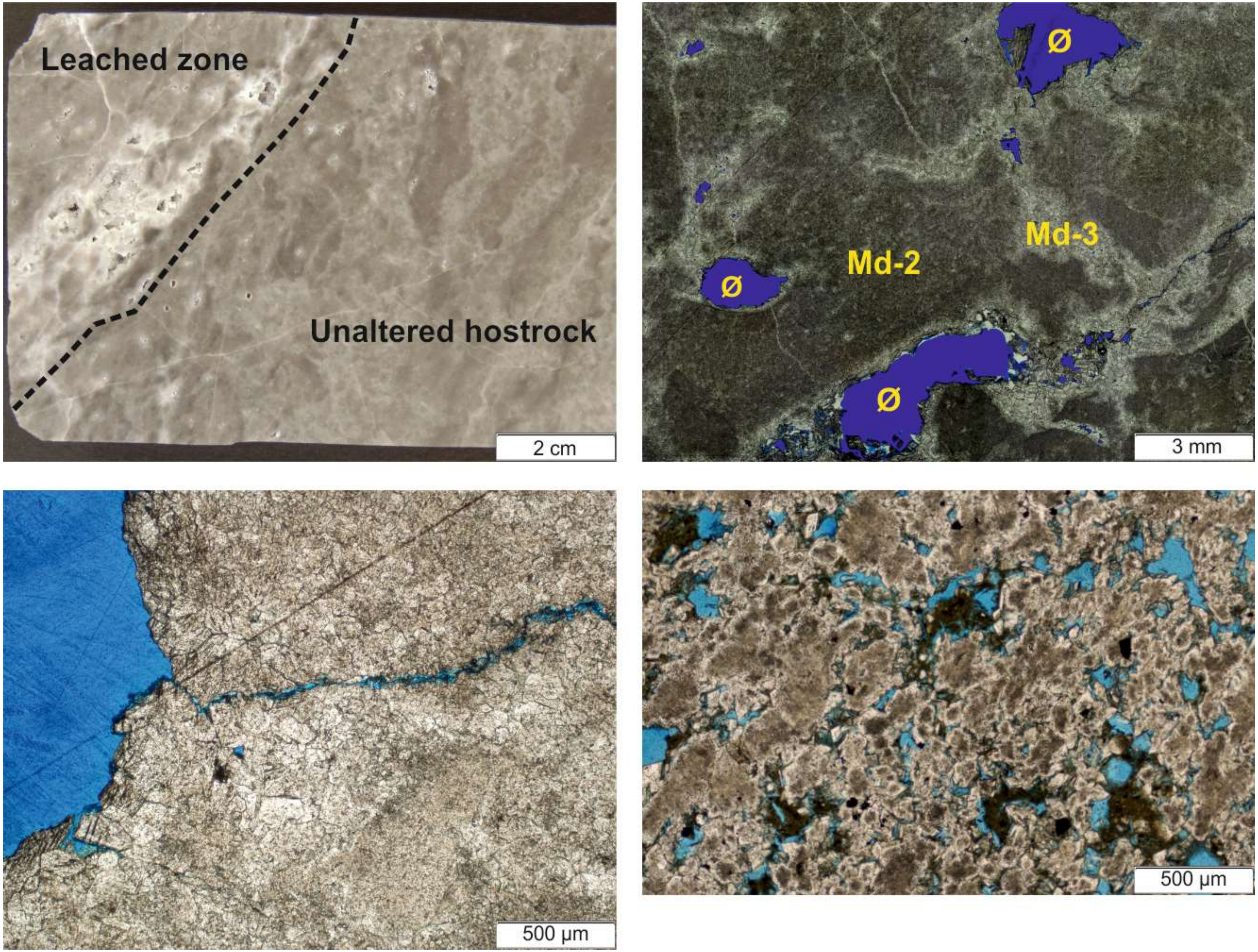

Late Cretaceous veins and vugs cemented by saddle dolomite

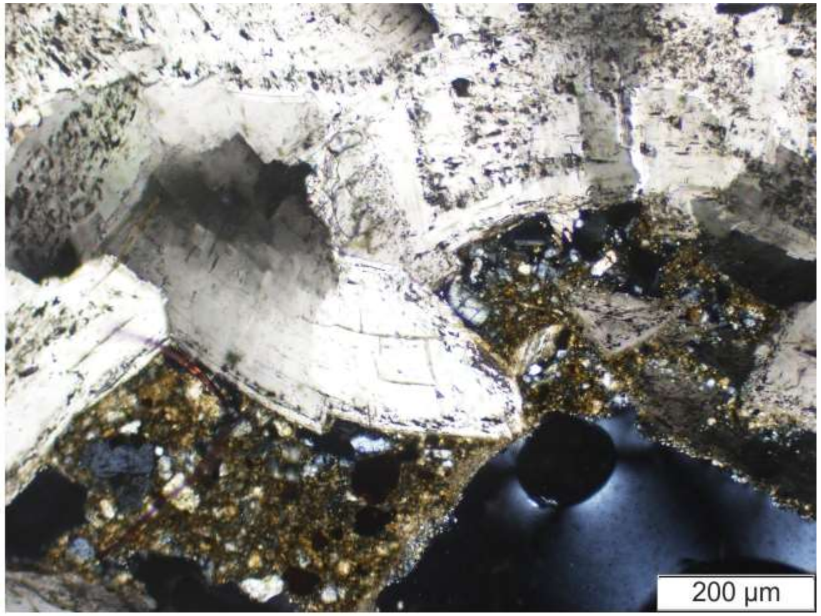

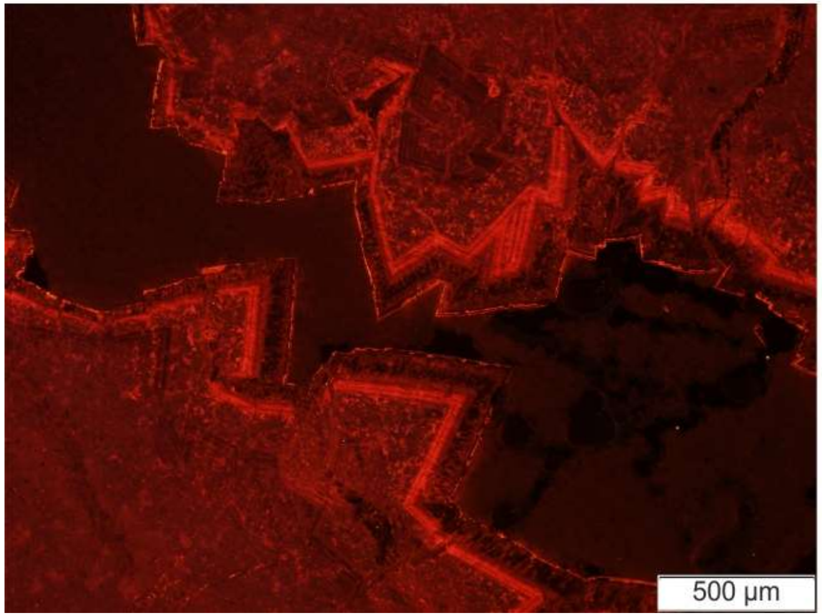

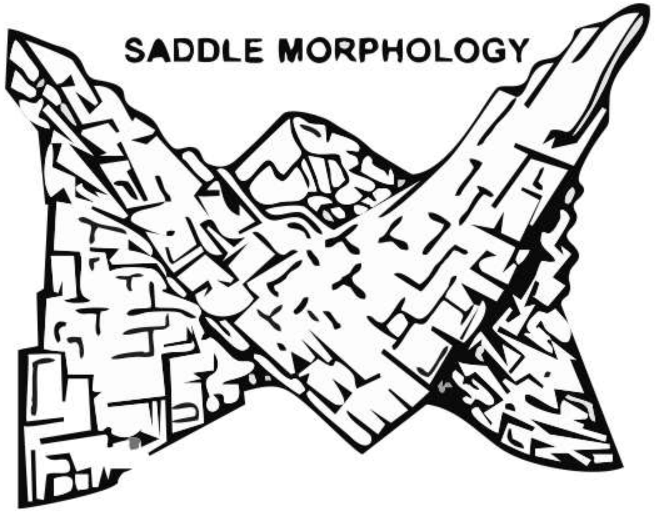

(After Davies and Smith 2006)

Porosity-reducing telogenetic cements

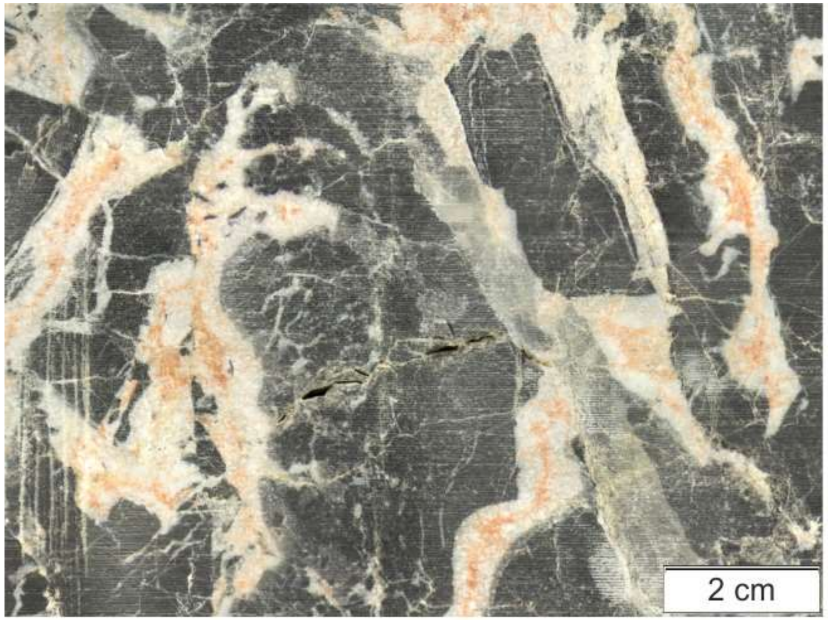

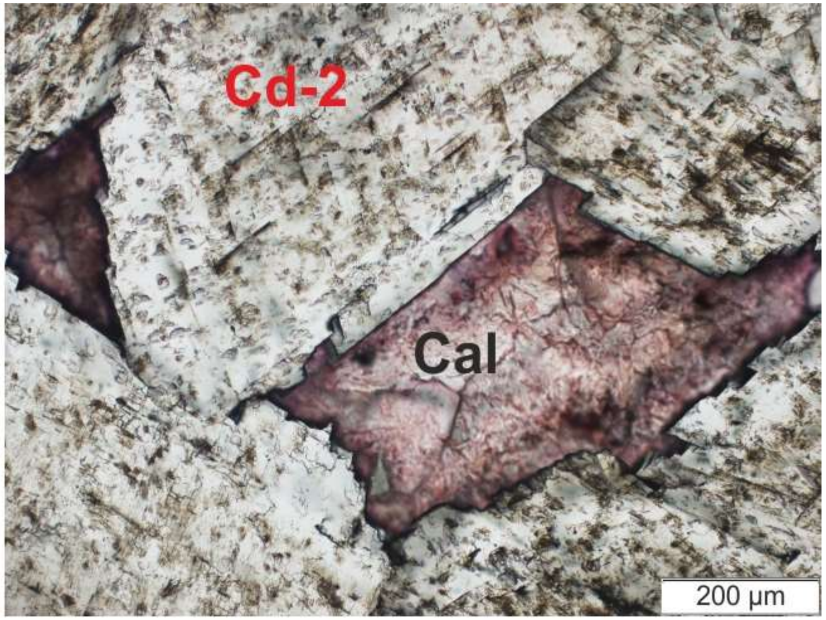

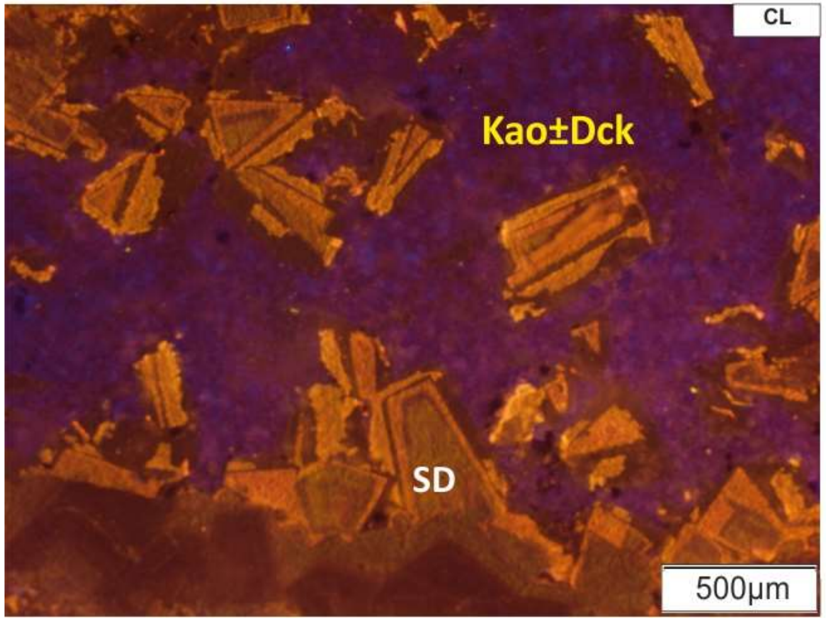

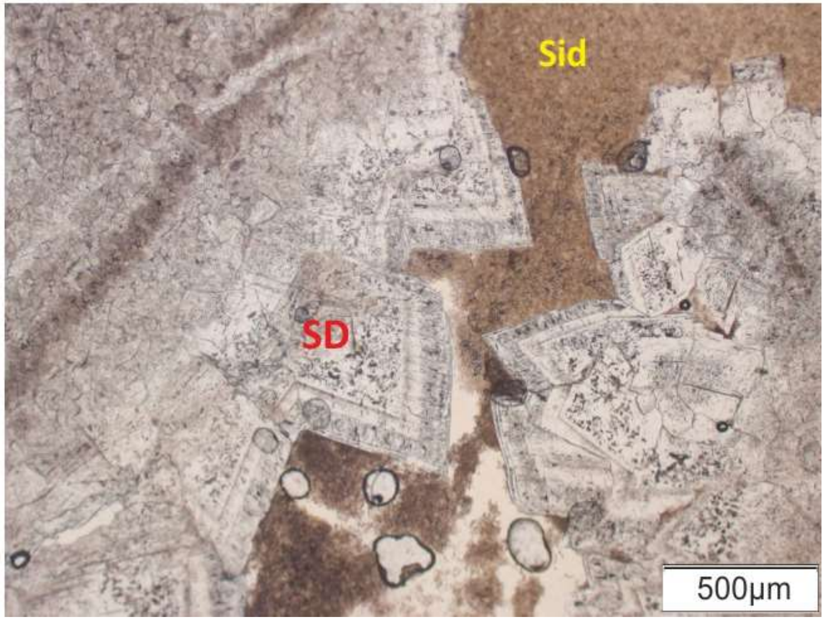

Neogene fractures and cements

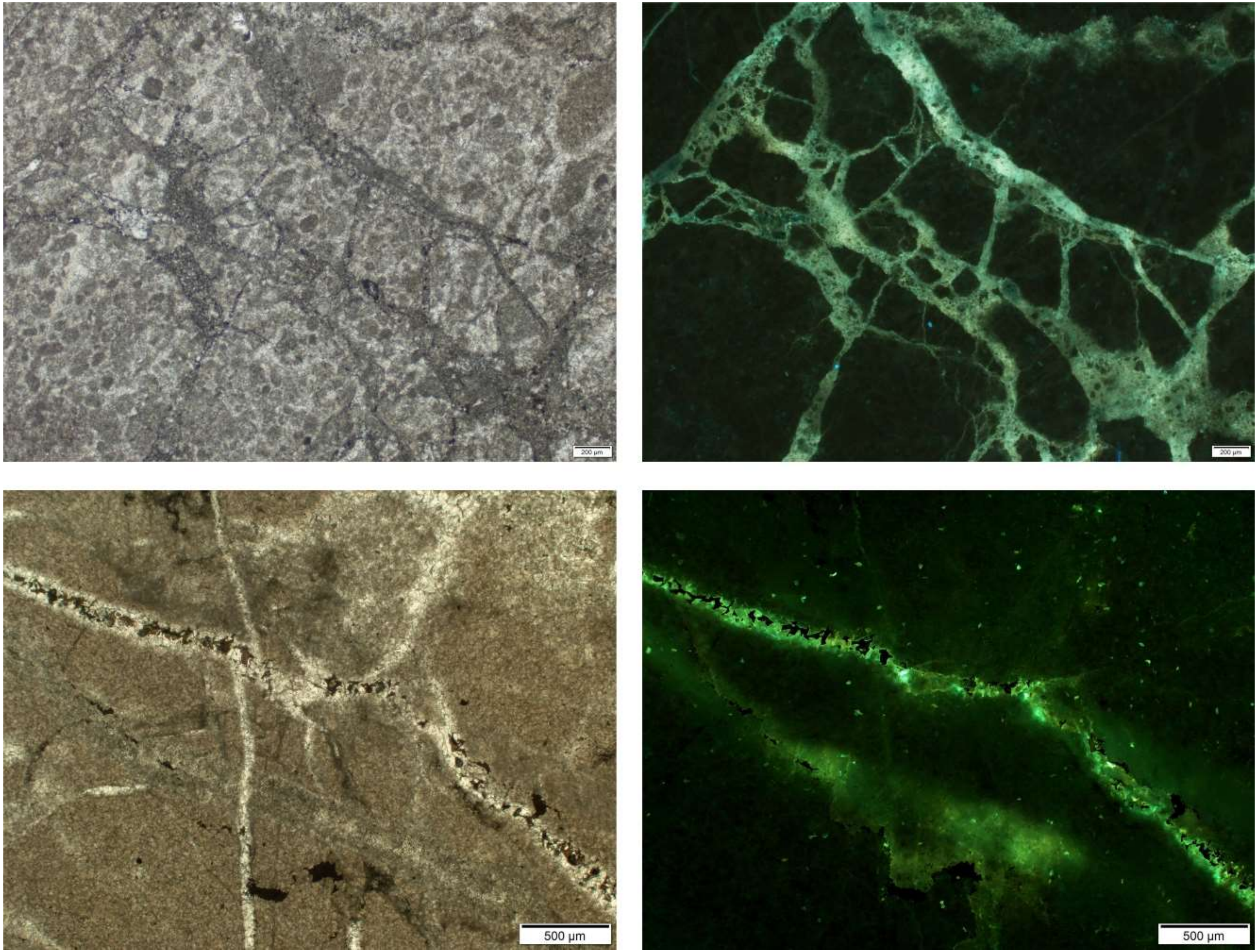

Carbon and oxygen isotopes

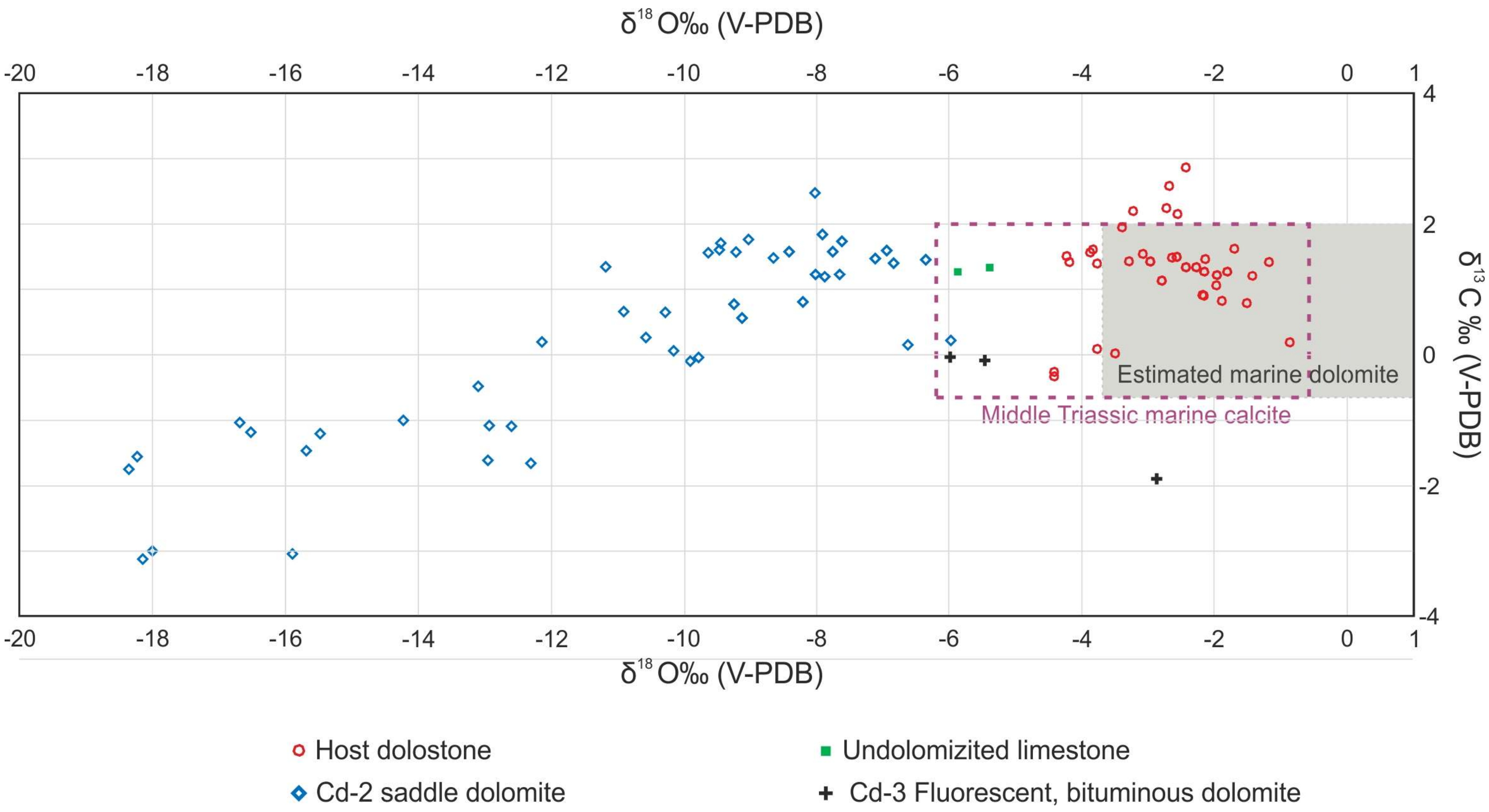

A cross-plot of $\delta^{13}C$ against $\delta^{18}O$ for different dolomites in the Szeged Dolomite Formation shown relative to fields of Middle Triassic marine calcite (Korte et al., 2005) and calculated (cf. Major et al., 1992) for cogenetic marine dolomite.

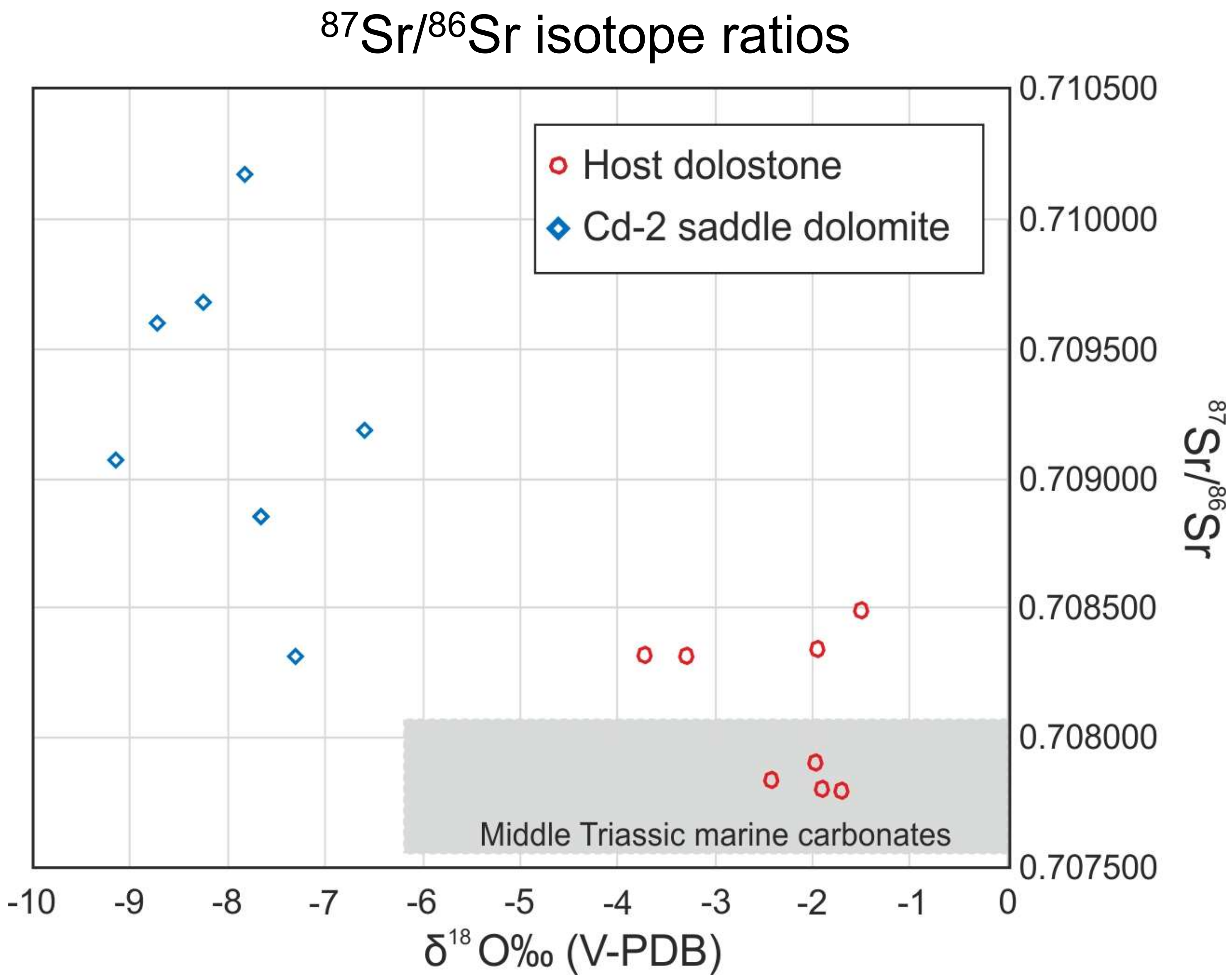

Fields depicted from the literature for the Middle Triassic marine calcite (Korte et al., 2003, 2005)

Fluid inclusion studies on saddle dolomite crystals

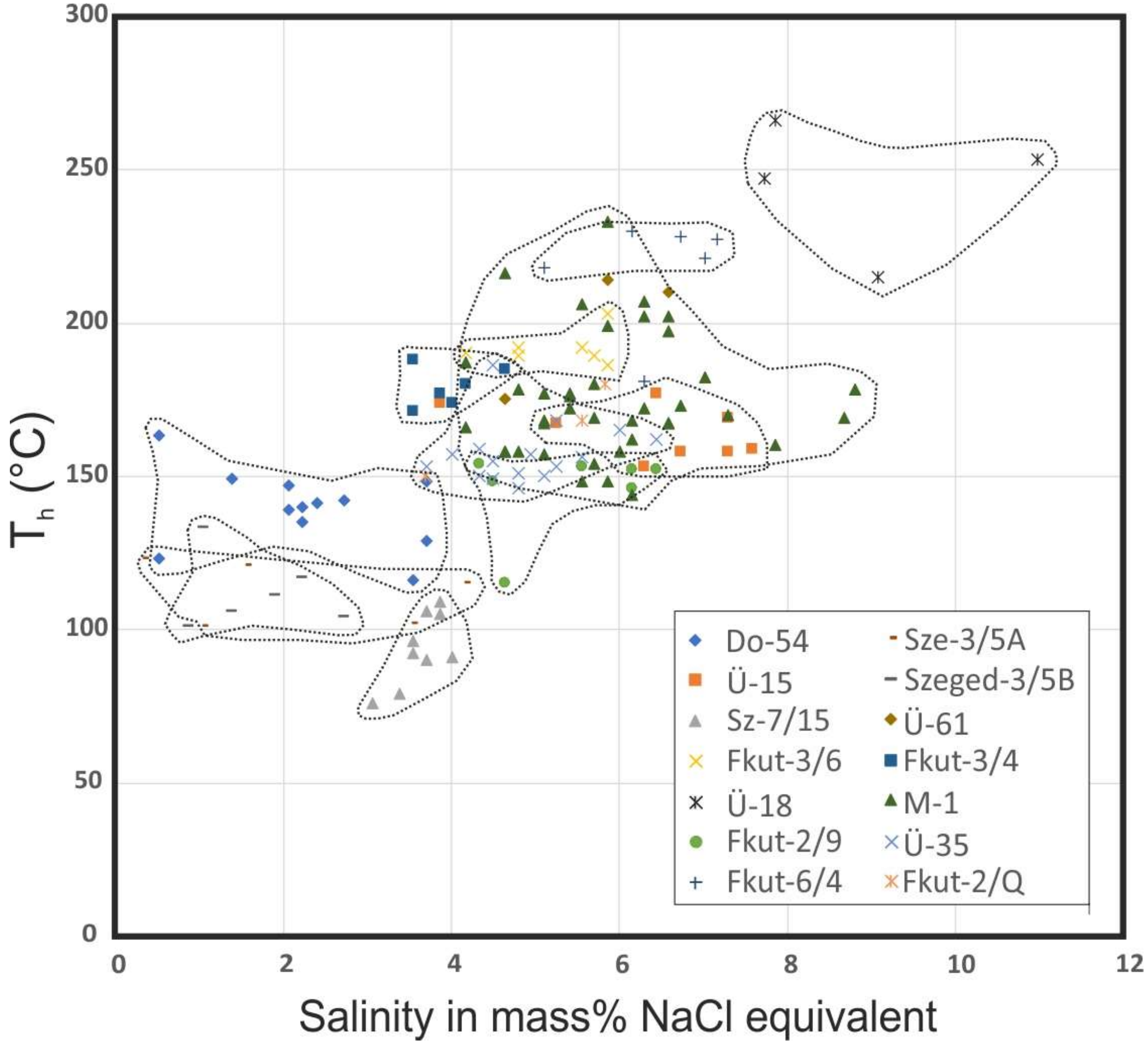

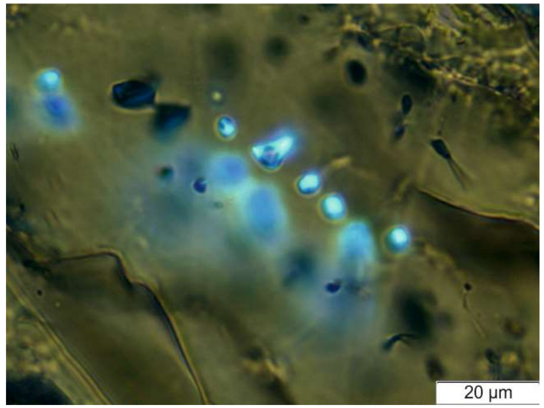

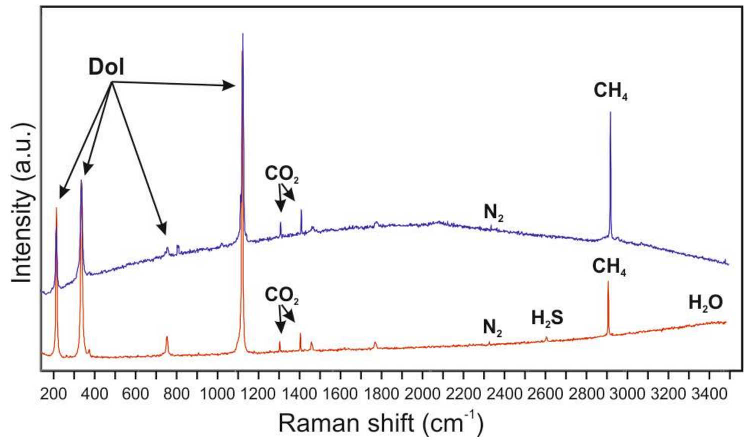

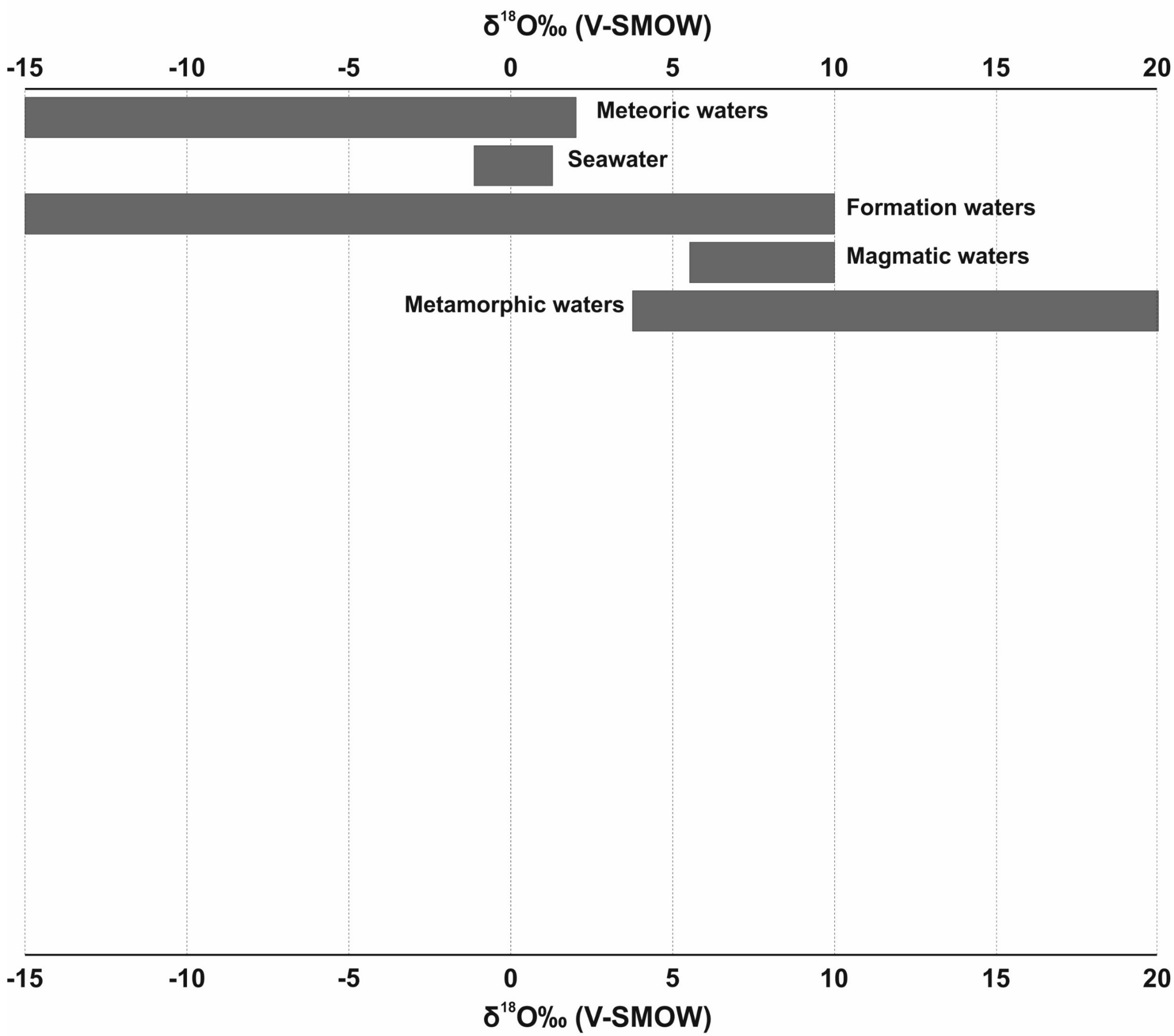

Calculated parent fluid composition based on the equation of Land (1985):

$$10^3 \ln \alpha_{dolomite-water} = 2.78*10^6T^{-2}+0.91$$

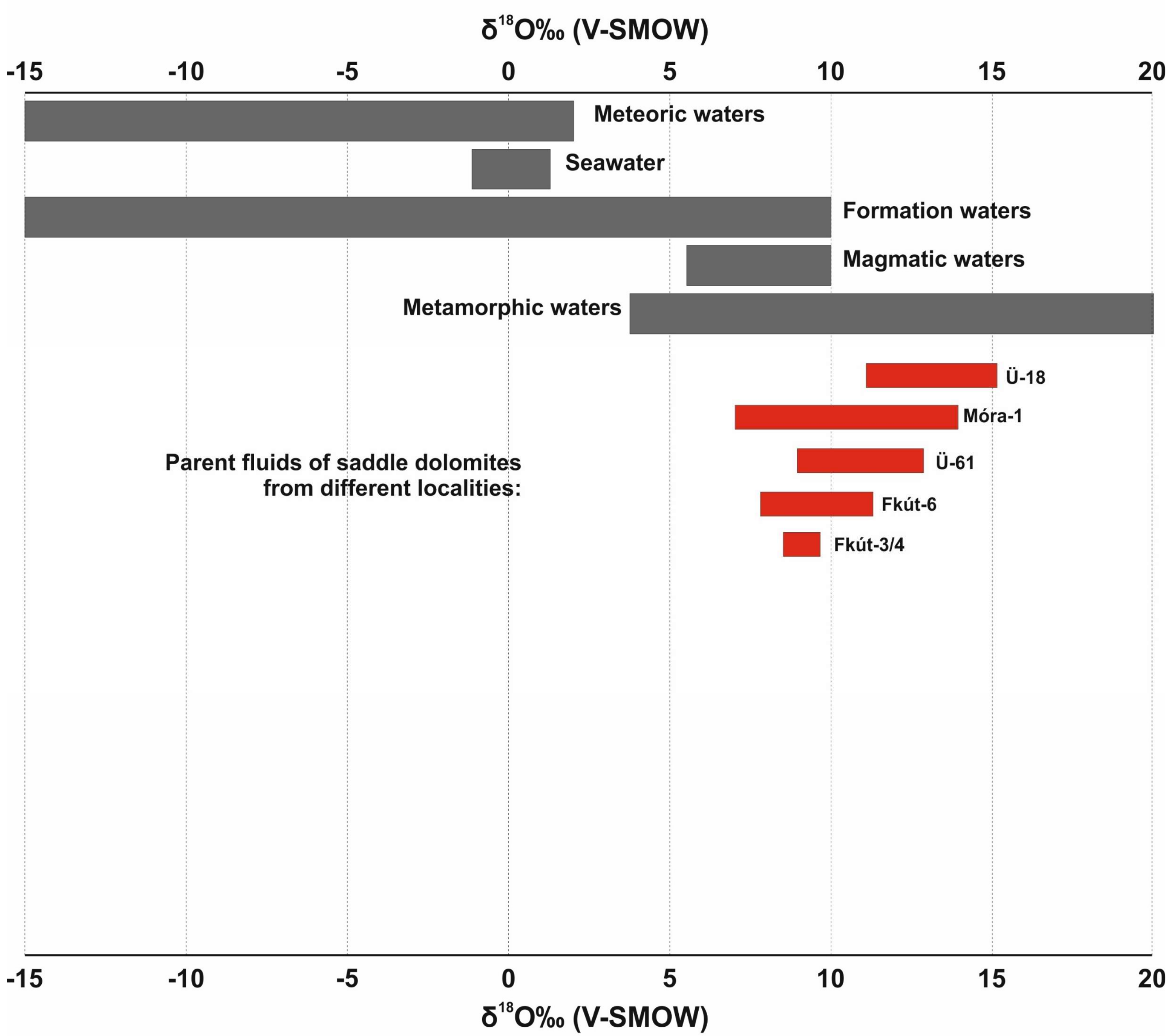

Calculated parent fluid composition based on the equation of Land (1985):

$$10^3 \ln \alpha_{dolomite-water} = 2.78*10^6 T^{-2} + 0.91$$

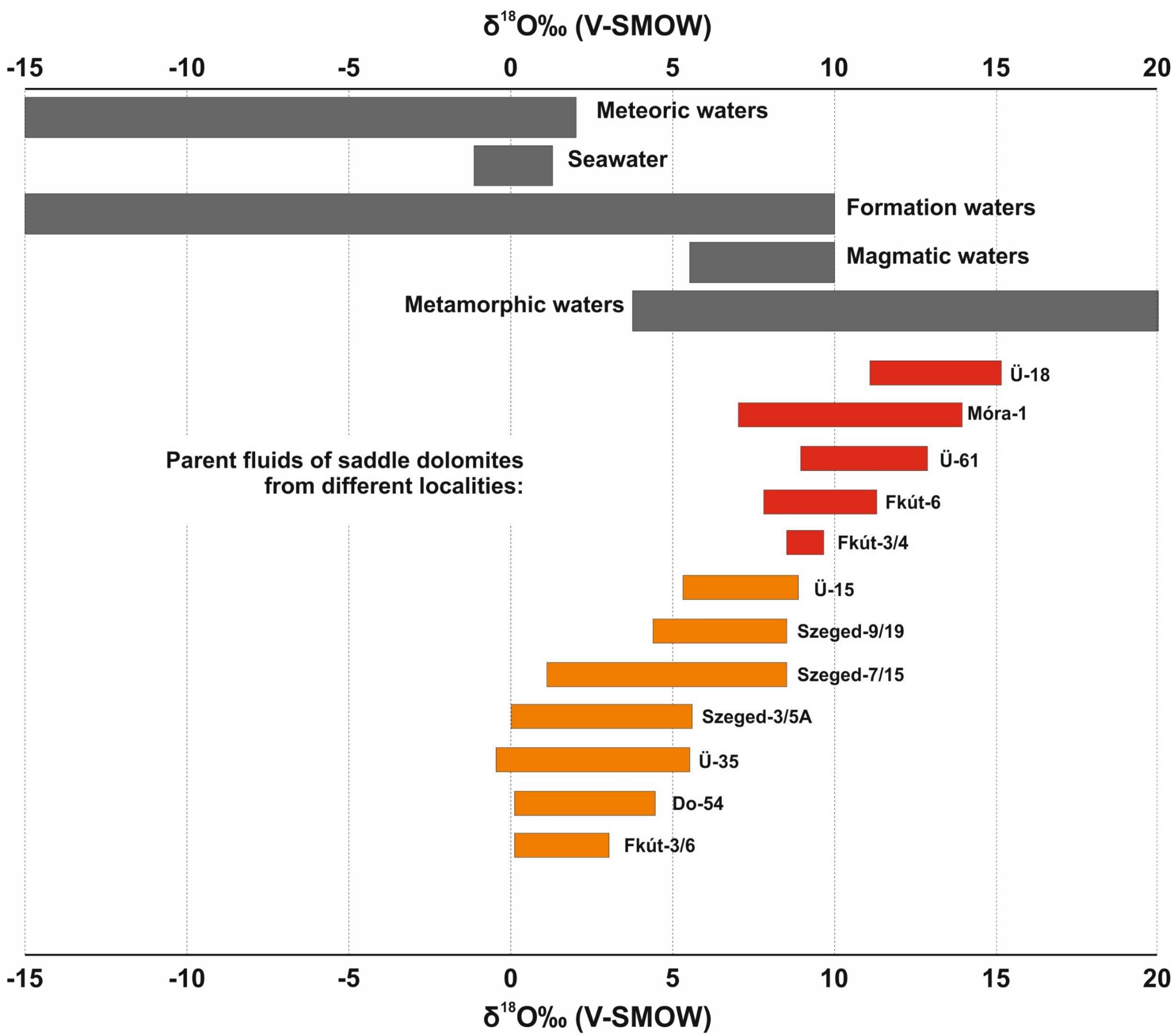

Calculated parent fluid composition based on the equation of Land (1985):

$$10^3 \ln \alpha_{dolomite-water} = 2.78*10^6 T^{-2} + 0.91$$

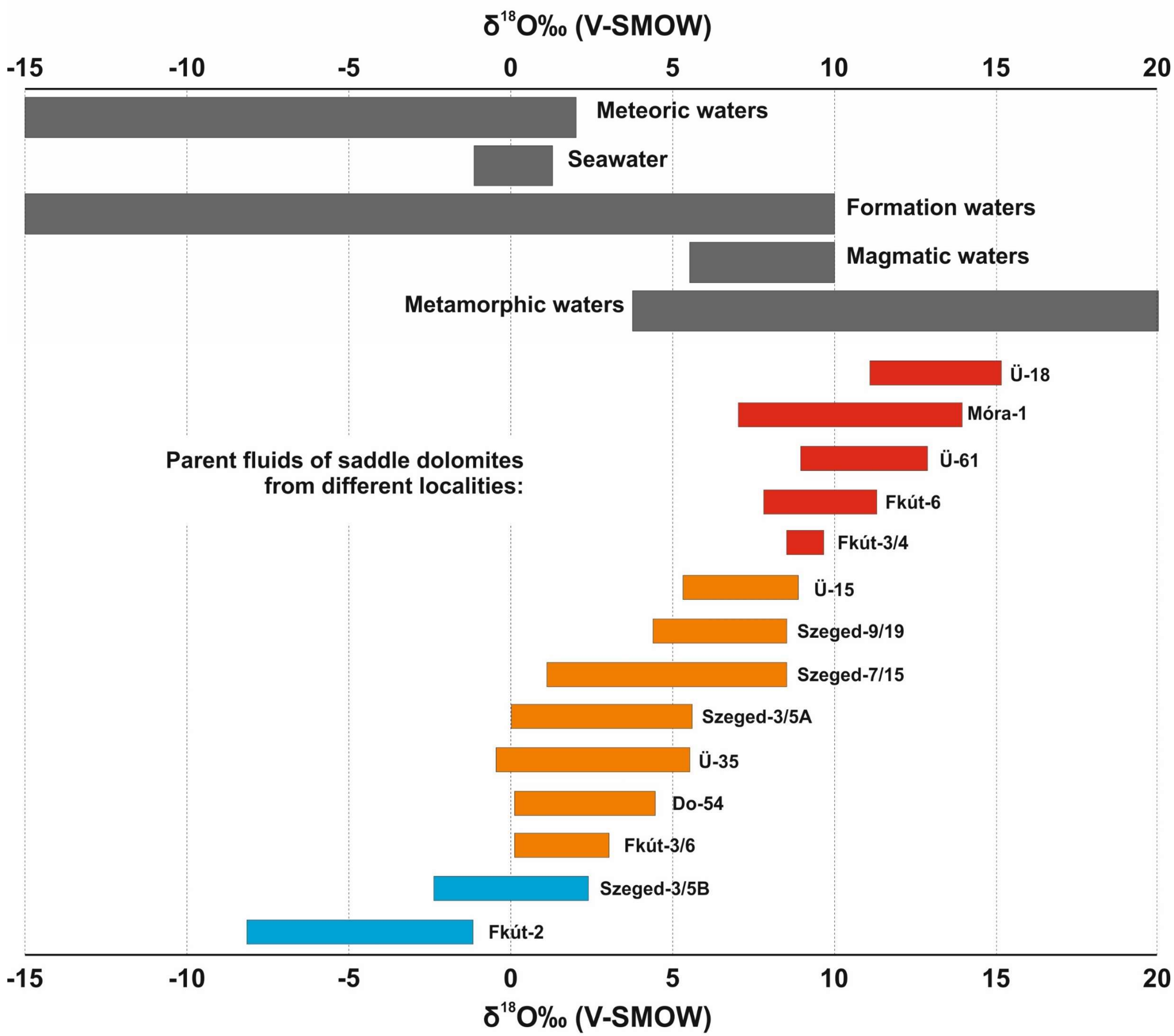

Calculated parent fluid composition based on the equation of Land (1985):

$$10^3 \ln \alpha_{dolomite\text{-}water} = 2.78*10^6 T^{-2} + 0.91$$

Hydrogen isotope composition of fluid inclusion-hosted H_2O

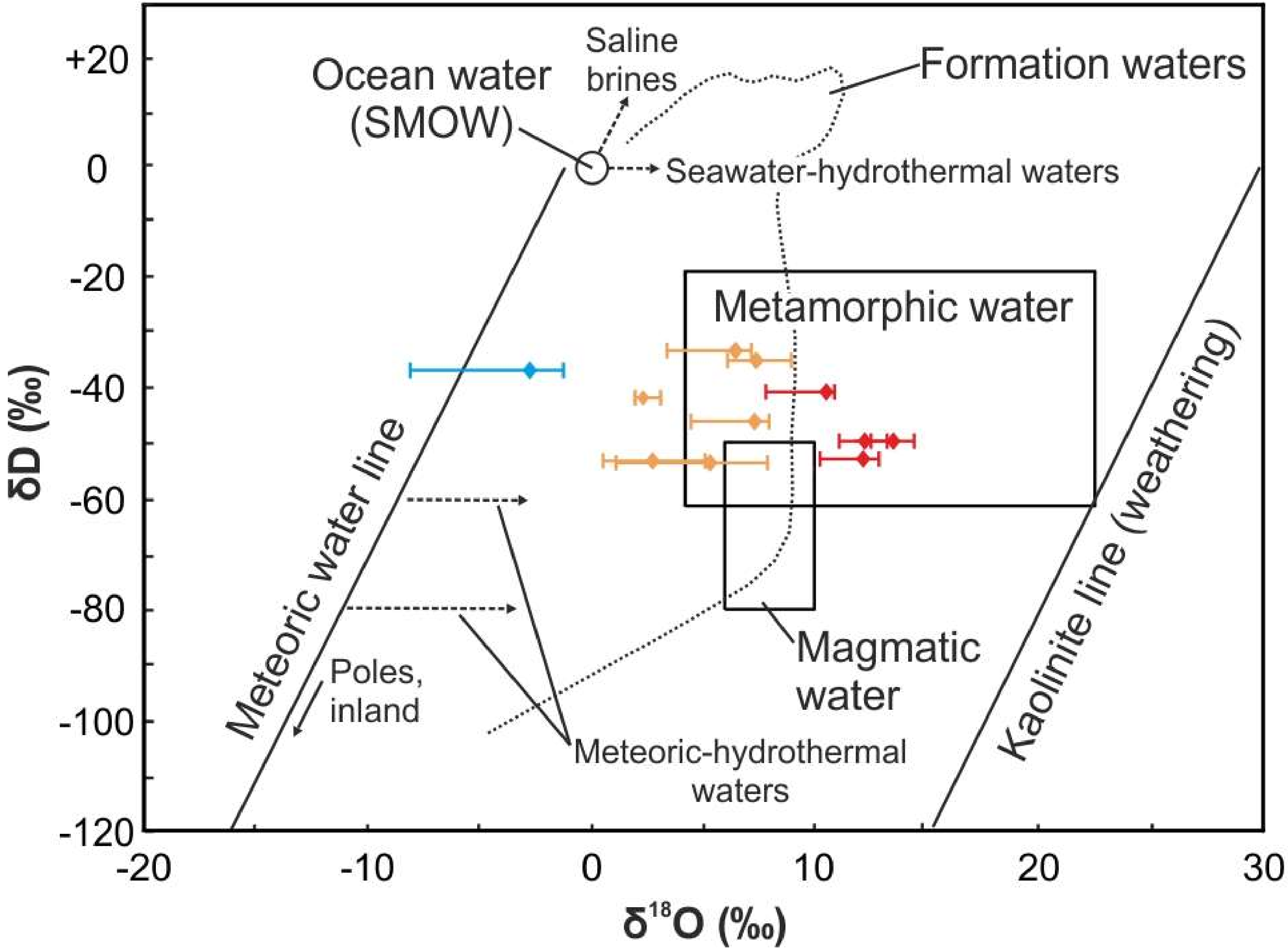

Fields of primary waters and transitions are from Sheppard (1986) and Hoefs (2004).

Note: the low and moderate salinity values paired with $\delta^{18}O_{H2O}$ data also support the mixed meteoric and metamorphic origin of fluids

Interpreted fluid inclusion data from saddle dolomite

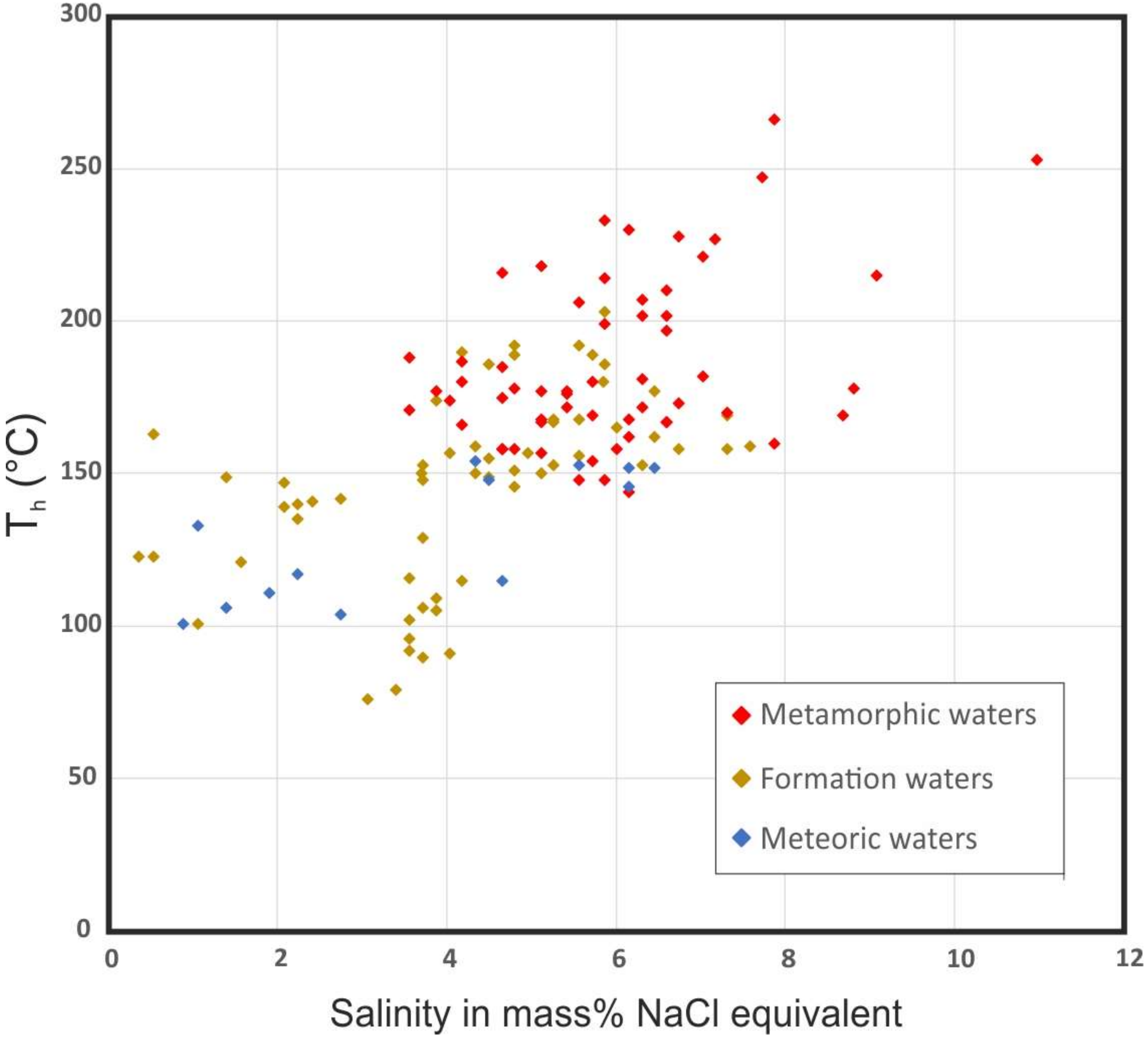

Available online at www.sciencedirect.com
SCIENCE DIRECT
ELSEVIER
Journal of Geochemical Exploration 78–79 (2003) 481–485
JOURNAL OF GEOCHEMICAL EXPLORATION
www.elsevier.com/locate/jgeoexp

Abstract

Fluid flow and diagenesis in carbonate dominated Foreland Fold and Thrust Belts: petrographic inferences from field studies of late-diagenetic fabrics from Albania, Belgium, Canada, Mexico and Pakistan

R. Swennen[a,*], H. Ferket[a], L. Benchilla[a,b], F. Roure[b], R. Ellam[c]
SUBTRAP team

[a] *Afd. Fysico-Chemische Geologie, K.U. Leuven, Celestijnenlaan 200C, B-3001 Heverlee, Belgium*
[b] *Institut Français du Pétrole, 1 et 4, av. de Bois-Préau, F-92852 Rueil-Malmaison, France*
[c] *Scottish Universities Environmental Research Centre, Rankine Avenue, East Kilbride, G75 0QF, Great Britain, UK*

Abstract

Five different Foreland Fold and Thrust Belt (FFTB) systems have been studied with the aim of reconstructing the fluid flow history through time and to deduce the primary processes affecting reservoir units. By placing the diagenetic history into its kinematic framework, a database is generated allowing to predict diagenetic processes in FFTBs. Particular attention is paid to the late diagenetic processes since petrographical and geochemical data indicate that several of these processes reflect nonequilibrium conditions with respect to their host rocks. Some of these systems involve channeled fluid flow where the system is, to some extent, water dominated (e.g. hydrothermal karstification, MVT mineralisation, zebra dolomitization and cooling of formation water). Other processes are less fluid prone, but here cooling of entire thrust sheets by thrusting and

Late Cretaceous syn-orogenic hydrologic system

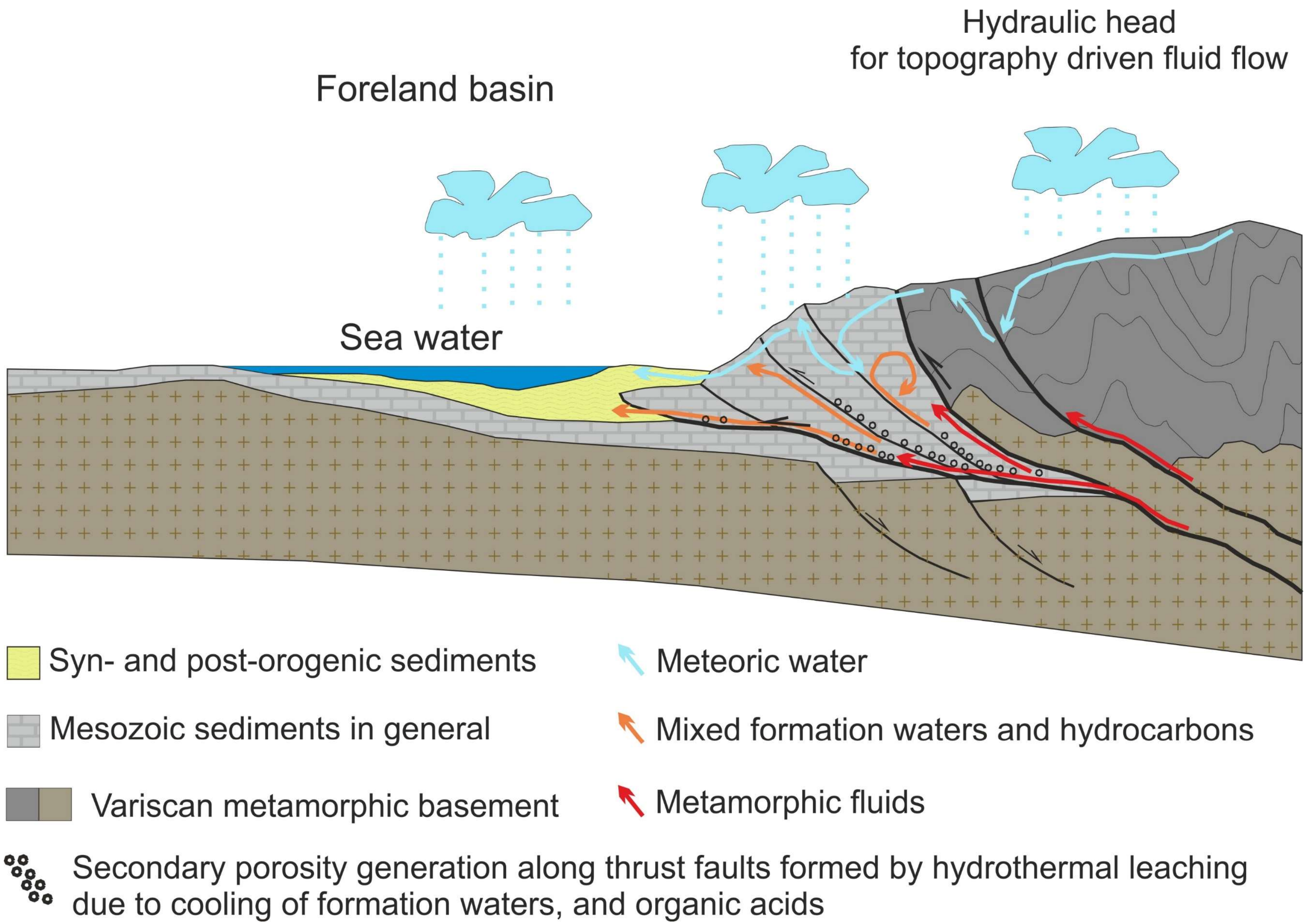

Schematic representation of fluid sources and pathways in a carbonate dominated fold-and-thrust belt (Based on Swennen et al. 2003 and Roure et al. 2005).

Paleogene erosion

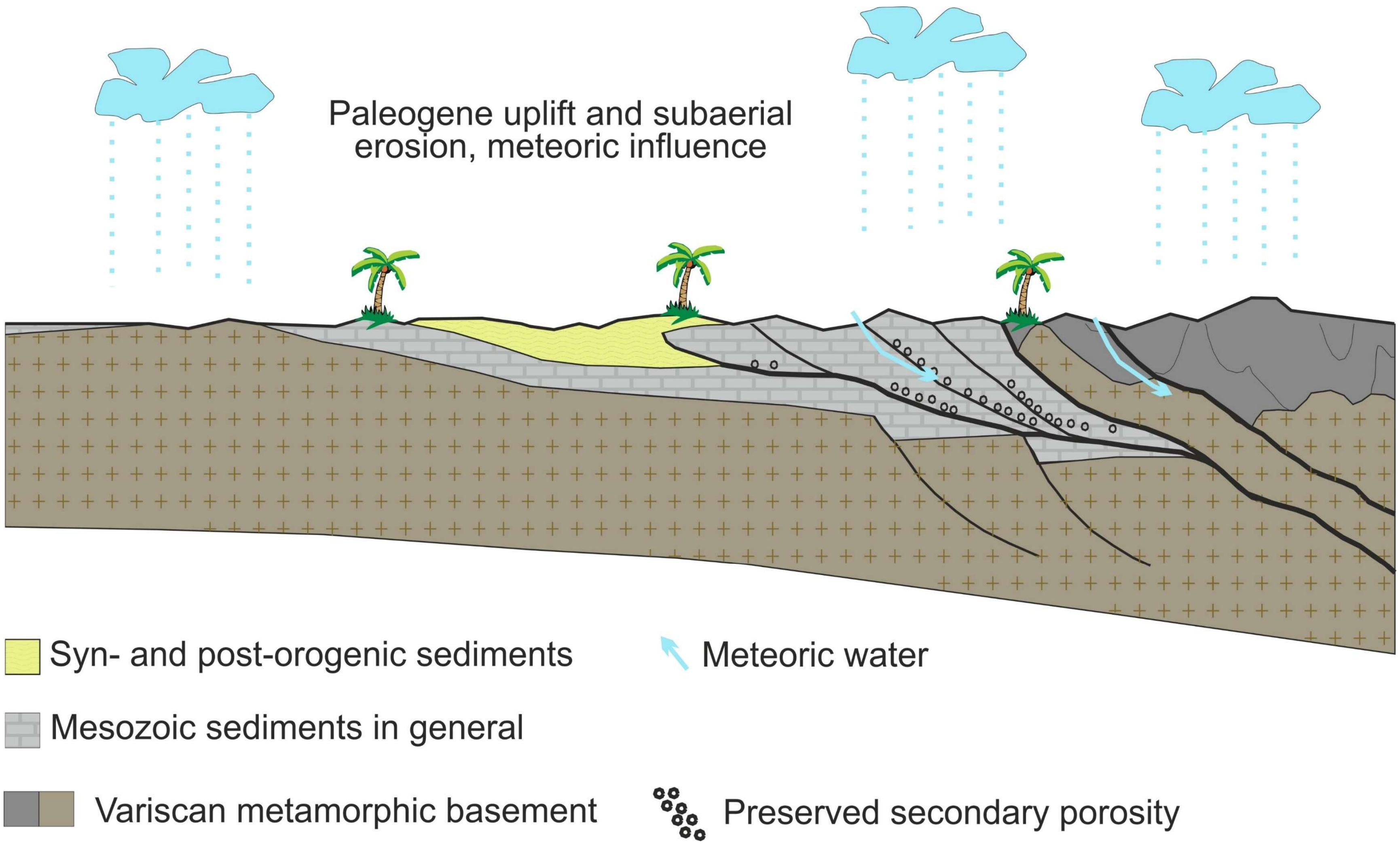

Formation of the recently known petroleum system during the Neogene

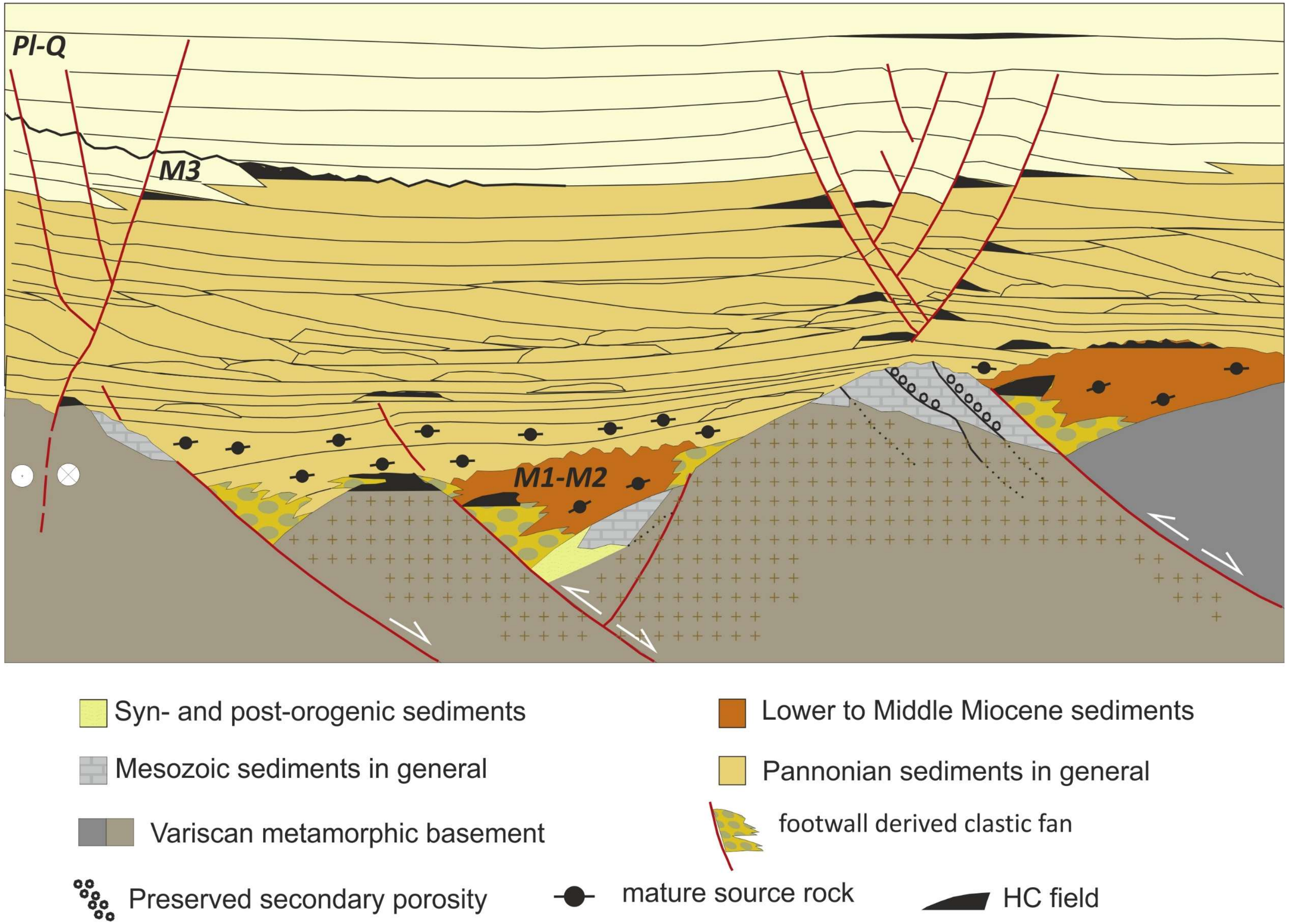

Idealized cross section showing the petroleum systems of the Neogene basin fill (modified after Balázs et al. 2017, and Tari & Horváth 2006).

Concluding remarks

- The main dolomitizing processes were controlled by the reflux of mesohaline seawater and/or deep convection of seawater through the ancient platform. These processes took place from the near surface to shallow burial realms and, by the time the succession reached the depth of up to 1000 meters, it was completely dolomitized and cemented.
- The saddle dolomites were formed through the hydrothermal alteration of matrix dolomite by way of invasion of metamorphogenic formational and meteoric fluids, that were probably channeled by the Upper Cretaceous subhorizontal overthrust zones during and immediately after the Alpine orogeny.
- The studied reservoir rocks contain significant amount of secondary porosity that were formed by the leaching effect of the hydrothermal fluids. These pores were partly occluded during the Paleogene–Middle Miocene subaerial exposure but their remarkable part could have been preserved, and currently serve as reservoir space.

Thank you for your kind attention!

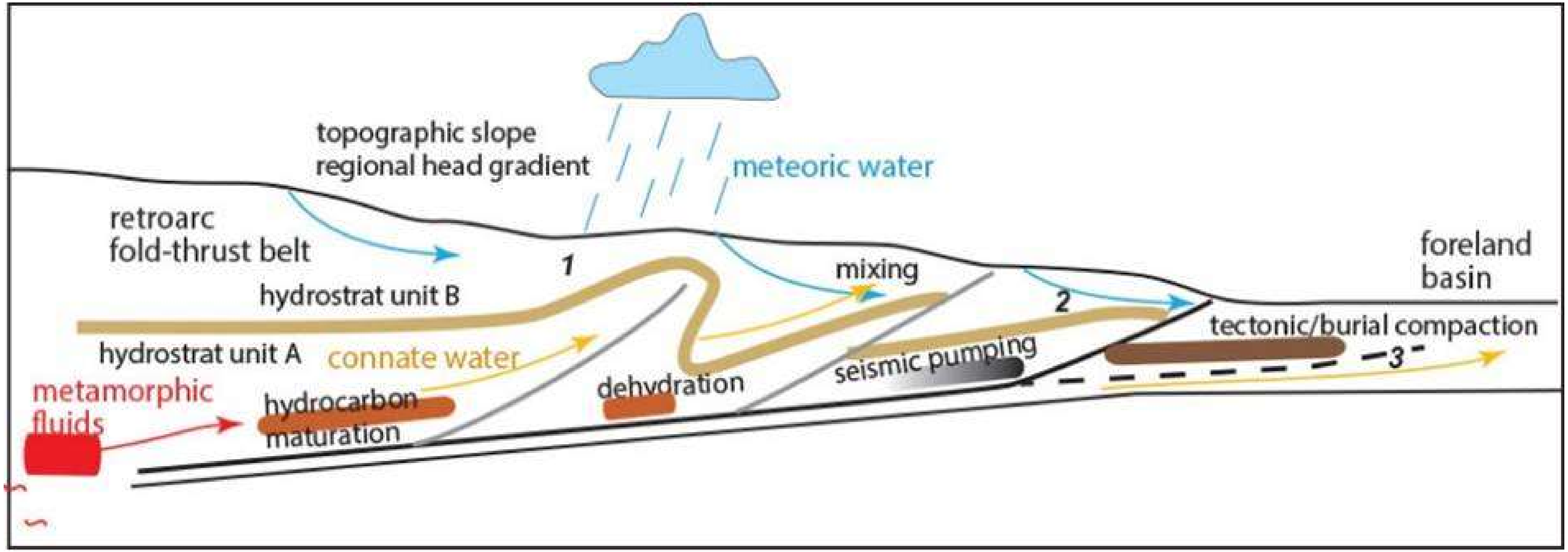
topographic slope
regional head gradient
meteoric water
retroarc
fold-thrust belt
foreland
basin
1
mixing
2
hydrostrat unit B
tectonic/burial compaction
hydrostrat unit A
connate water
seismic pumping
3
metamorphic
fluids
hydrocarbon
maturation
dehydration

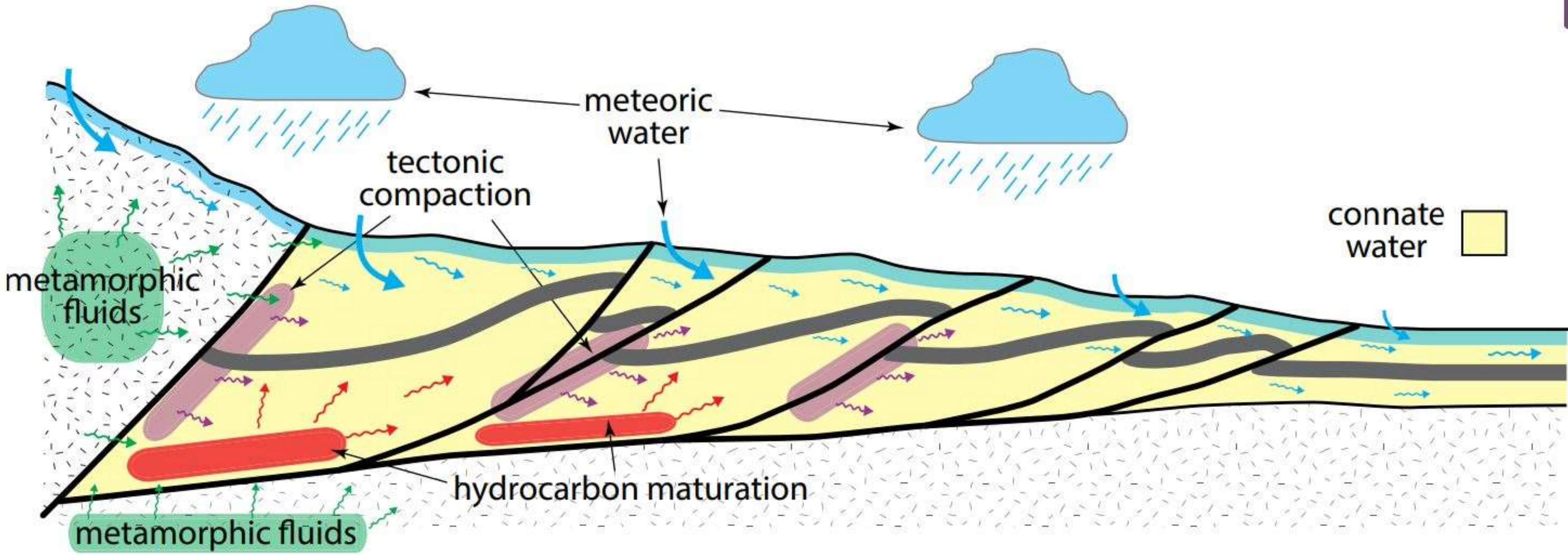

Figure 1. Generalized illustration of fluid system structure within a foreland orogenic wedge; colors represent different fluid types and origins.

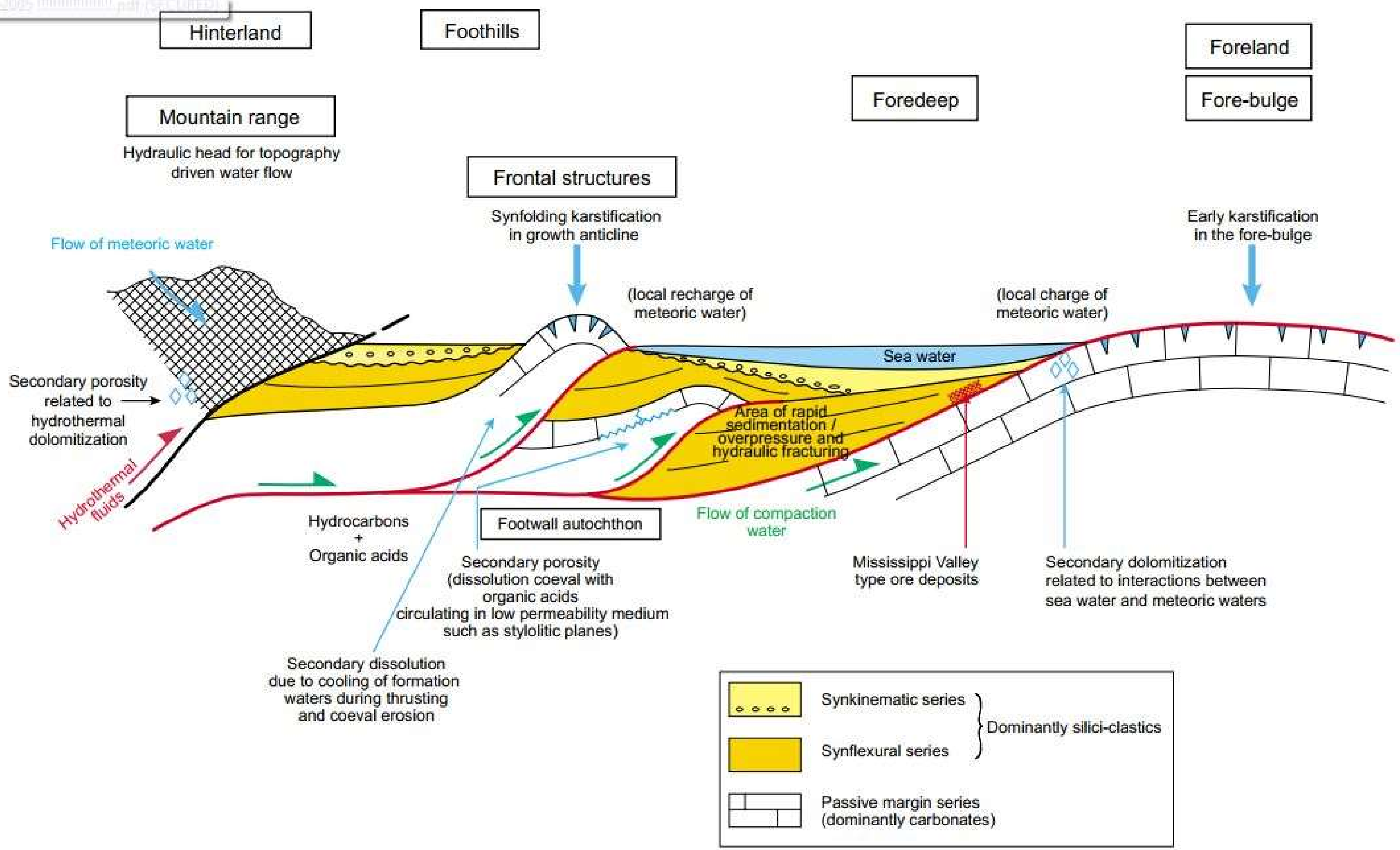

Figure 2

Synthetic cross-section of a foreland fold-and-thrust belt summarizing the main structural domains, as well as the various cementation habitats *versus* dissolution of carbonate reservoirs.

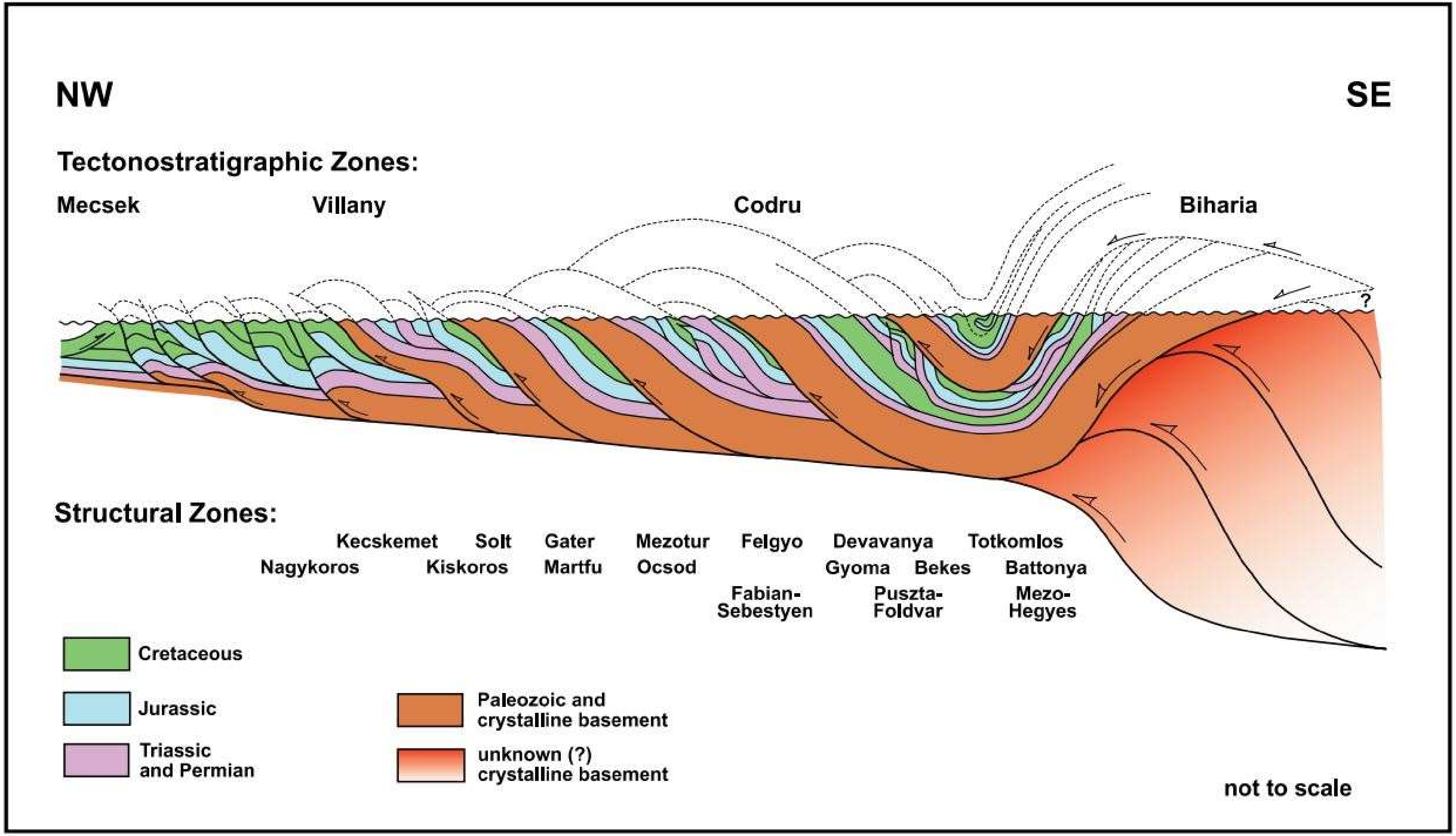
NW
SE
Tectonostratigraphic Zones:
Mecsek
Villany
Codru
Biharia
?
Structural Zones:
Kecskemet
Solt
Gater
Mezotur
Felgyo
Devavanya
Totkomlos
Nagykoros
Kiskoros
Martfu
Ocsod
Gyoma
Bekes
Battonya
Fabian-Sebestyen
Puszta-Foldvar
Mezo-Hegyes
Cretaceous
Jurassic
Triassic and Permian
Paleozoic and crystalline basement
unknown (?) crystalline basement
not to scale

Depth related δ^{18}O and T_h data measured on Cd-2 dolomite crystals

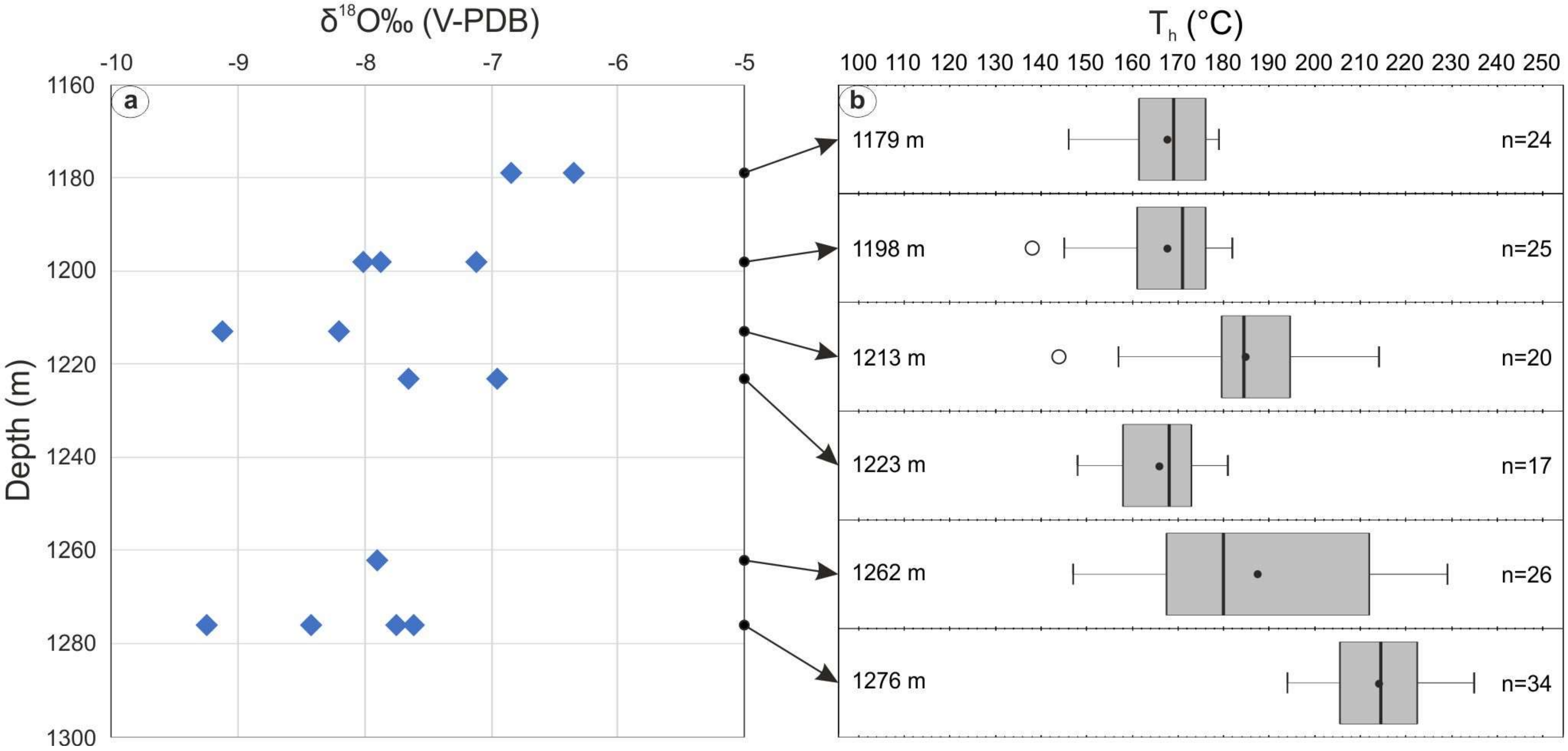

The T_h data for the six measured Cd-2 dolomite samples fall along a line of slope average 30–50°C/100 m which suggest an extremely increased heat-flow that could be interpreted as a result of a **relatively short-term hydrothermal overprint**.

The δ^{18}O values measured from the same samples change simultaneously with the T_h data that suggests an **equilibrium isotope fractionation during the precipitation**.

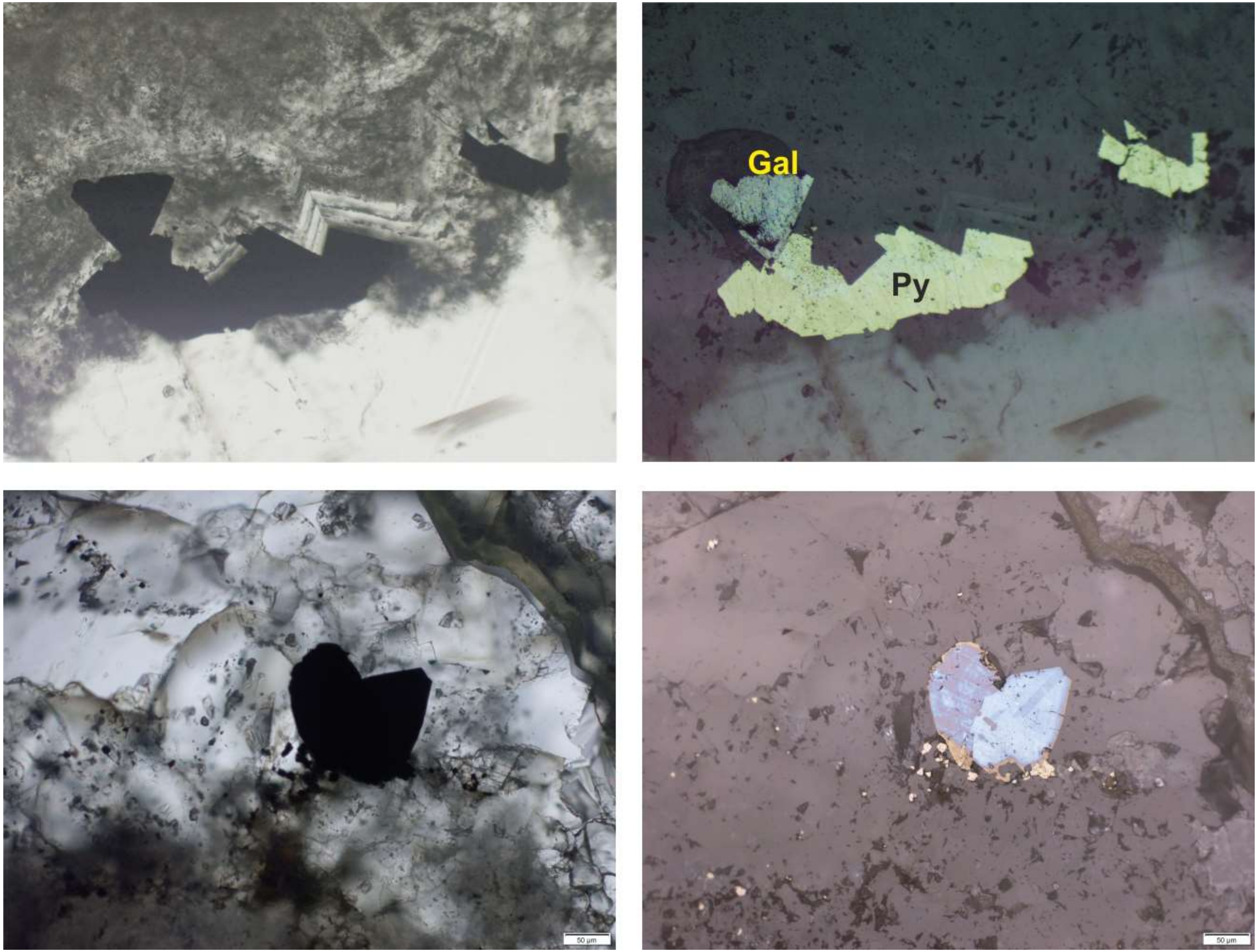
Gal
Py

Pervasive early diagenetic dolomitization

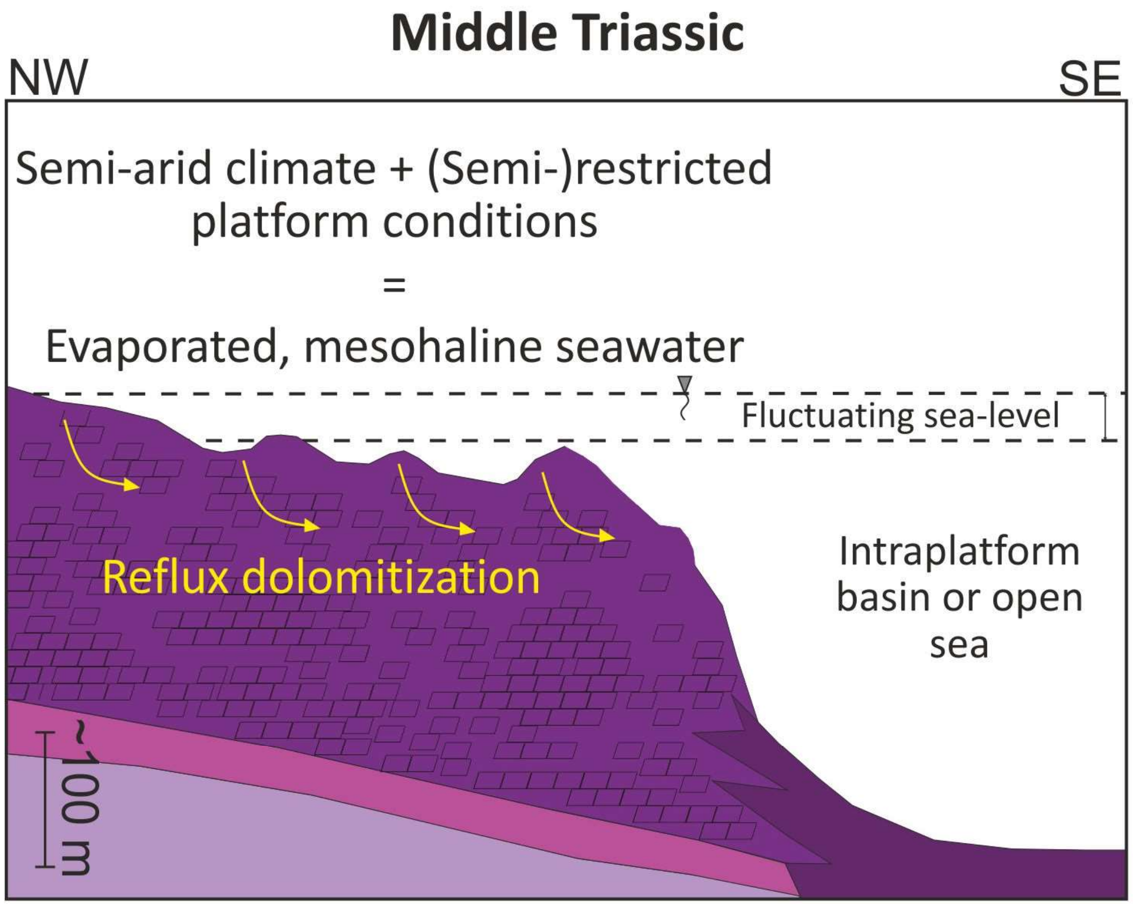

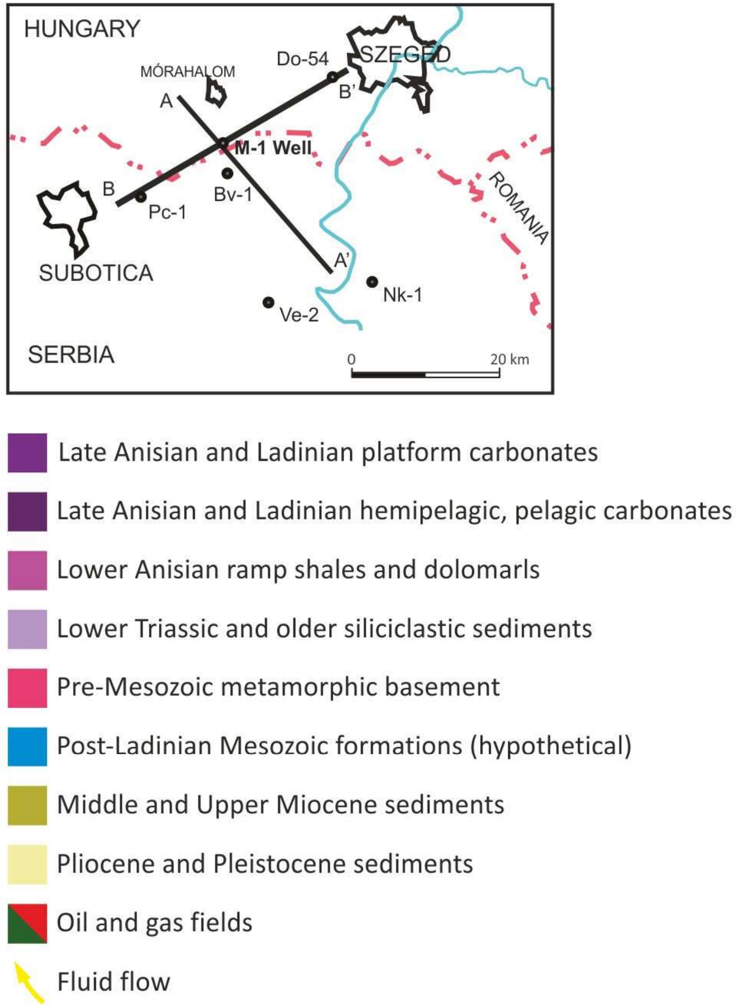

<u>'Seawater dolomitization' model</u>:
reflux of slightly evaporated seawater and minor overprint by thermal seawater convection (e.g., Whitaker et al., 1994; Machel, 2004).

Hydrothermal alteration

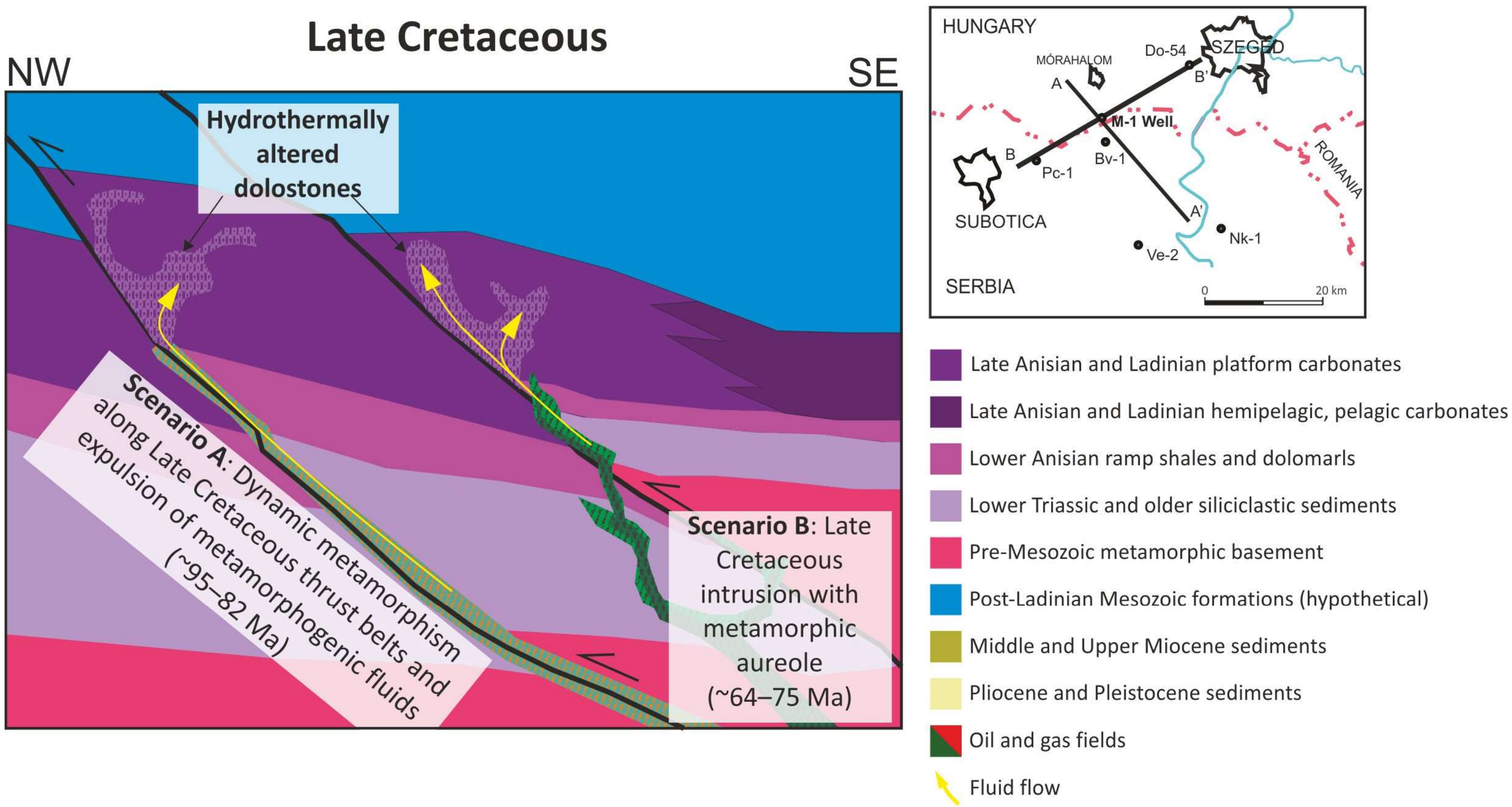

Possible timing of metamorphic and/or magmatic fluids:
Turonian–Coniacian (Pre-Gosau) nappe-stacking and/or subsequent calc-alkaline intrusive magmatism (‚banatite’) during the Campanian–Maastrichtian.

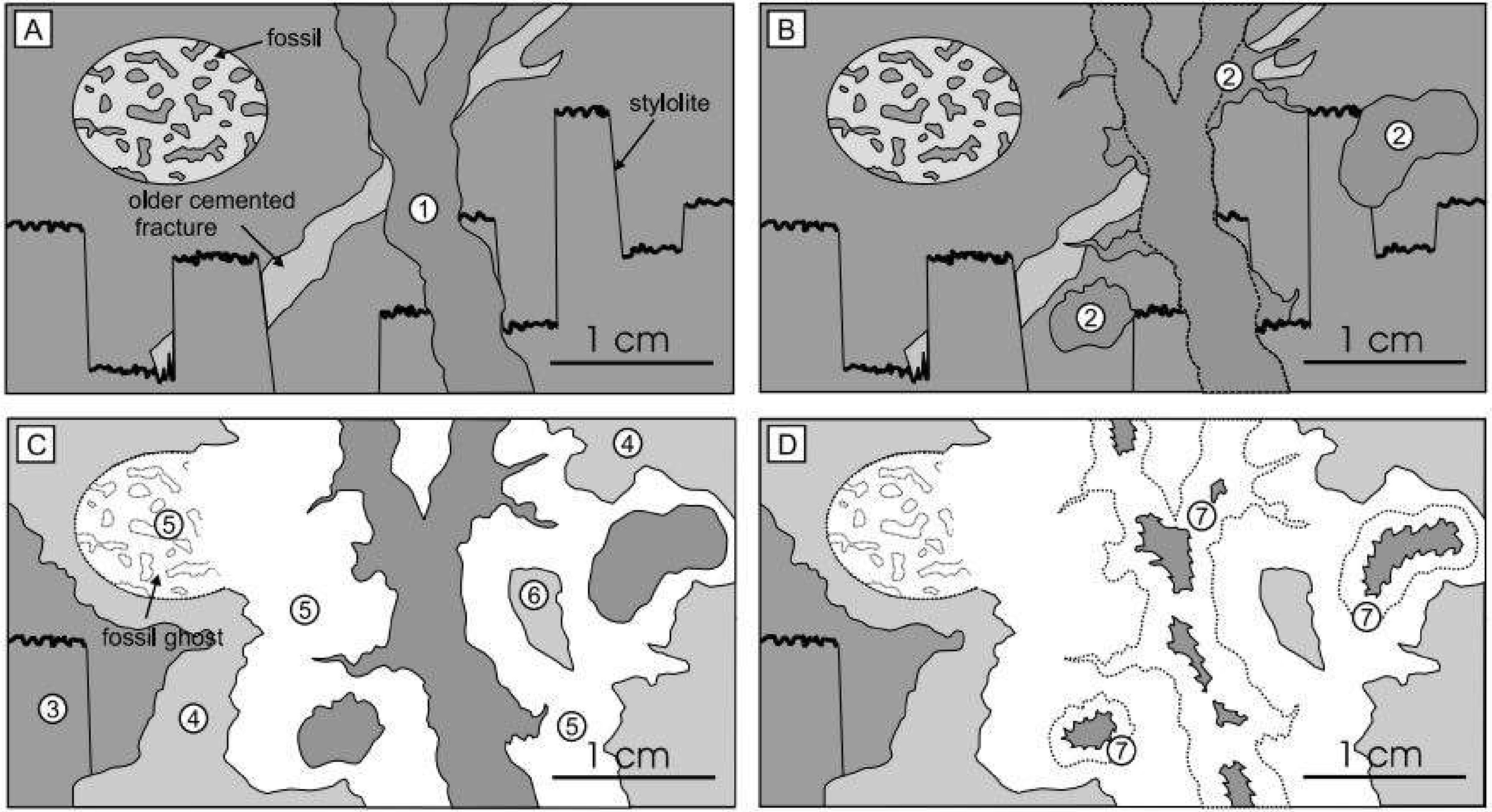

Figure 12. Schematic representation of dolomitization and subsequent hydrothermal alteration, based on petrographic observations. Precursor limestone, including cements of phase 6 in the narrow fracture, was previously replaced by GMD (phase 10, Figure 4), whereas the calcite skeleton of fossil was not replaced. (A) Vertical to subvertical fracture (1) (fracture II, phase 12, Figure 4) cut across all previously formed diagenetic phases. Some dissolution along the fracture walls exists, resulting in irregular boundaries caused by the introduction of a solution undersaturated with respect to dolomite. (B) The hydrothermal fluid undersaturated with respect to dolomite continues to dissolve dolomite adjacent to the walls of the fracture and in adjacent permeable domains. Dissolution by the hydrothermal fluid resulted in an increase in the width of the fractures and the generation of oversized pores = vugs (2). (C) Continued dissolution brings the hydrothermal fluid to saturation with respect to dolomite. At this stage, dissolution ceases and replacive saddle dolomite (5) forms immediately adjacent to the fracture walls and oversized vuggy pores. At greater distances away from the conduits for the hydrothermal fluids, the original gray matrix dolomite shows textural and/or geochemical evidence for recrystallization (4, reX GMD). Another product of the recrystallization of gray matrix dolomite is the generation of pseudobrecciated dolomite fabrics (6). In domains where the hydrothermal fluids did not enter, there is no textural and/or geochemical evidence for recrystallization of gray matrix dolomite (3). (D) The latest stage of hydrothermal alteration is represented by the partial cementation of oversized pores and fractures by well-developed crystals of saddle dolomite (7) (SD, phase 13, Figure 4).

BOX 1.13 Two end member models of metamorphogenic ore formation

1. Prograde metamorphogenic ore formation. Normally, metamorphic fluids are expulsed in the form of a wide and diffuse flow into regions of lower pressure (Hanson 1997, Jamveit & Yardley 1997). Large regional tectonic structures (shear zones, extensional faults and thrust faults) focus the diffuse flow, because they can be channels of higher permeability (Figure 1.85). The permeability of the lower ductile crust (~10–15 km beneath the surface, depending on the geothermal gradient) undergoing prograde metamorphism is very low with a flow of only 0.25 m/year (Beaudoin & Therrien 1999) and the pressure regime is lithostatic. Note, however, that even in the middle and lower crust, an interplay between brittle and ductile deformation may occur (Mancktelow 2006). In the brittle upper crust, permeability is much higher and flow in faults reaches 100–1000 m/year. When rising fluids enter this regime, pressure is released and approaches hydrostatic conditions. Descending (e.g. meteoric) water can penetrate as far as the brittle/ductile boundary (Ingebritsen & Manning 1999). Because of these particular conditions, the brittle/ductile transition at ca. 425–375°C is a very frequent location of metamorphogenic ore deposit formation.

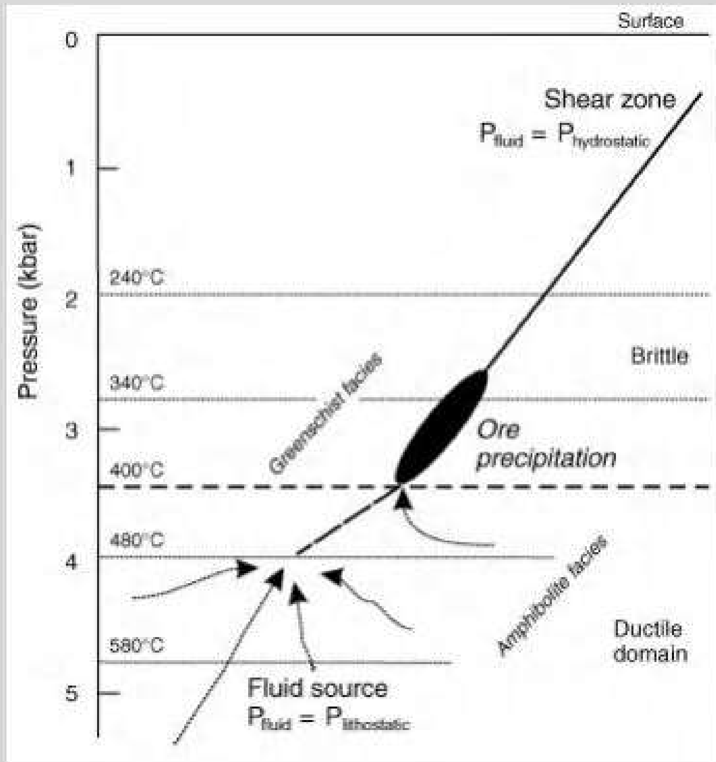

Figure 1.85 Ore deposit formation by prograde metamorphism. A shear zone focuses upflow of metamorphic fluids because of higher permeability. Its crustal-scale vertical extent facilitates transfer of fluids from lithostatic to hydrostatic pressure domains. Ore formation is a consequence of chemical or physical traps. The system is open, the mass flow is unidirectional.

2. Retrograde metamorphogenic ore formation. Many geological observations (e.g. concerning the structural control of orebodies) indicate that ore formation took place long after peak metamorphic conditions (or even totally unconnected to


200 µm

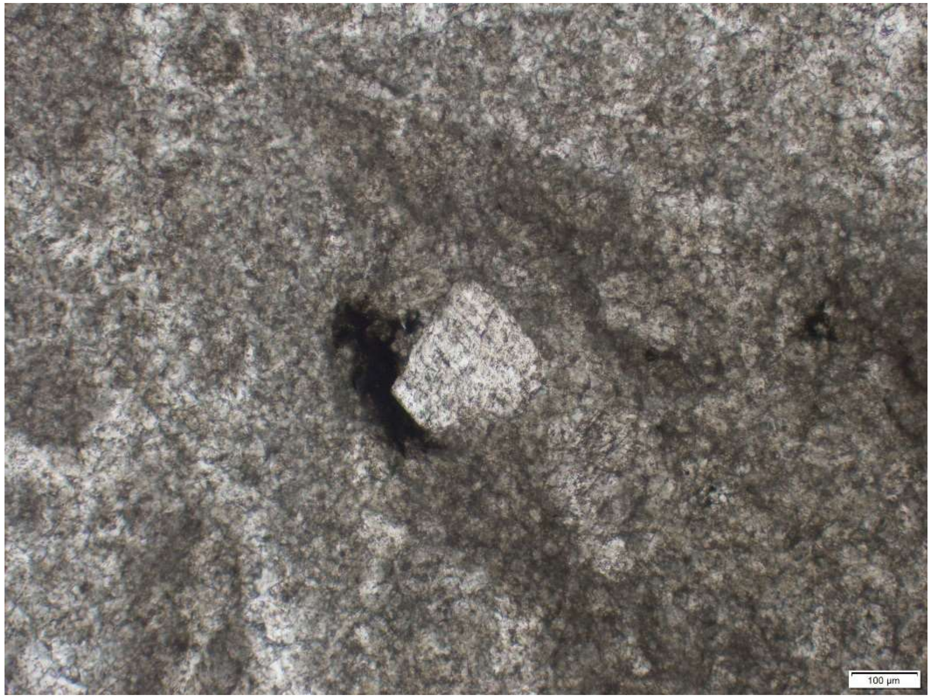
100 µm